ISSN 2303-4521
Periodicals of Engineering and Natural Sciences *Methodology/Method*
Vol. 9, No. 4, September 2021, pp.214-241

Mathematical modelling and development of a computational algorithm for the study of thermo-stressed state of a heat-resistant alloy

Beket Kenzhegulov [1], Raigul Tuleuova [1], Aigul Myrzasheva [1], Nurgul Shazhdekeyeva [1 *], Galymzhan Kabylkhamitov [1]
[1] Department of Mathematics and Methods of Teaching Mathematics, Kh. Dosmukhamedov Atyrau University

ABSTRACT

The problem of increasing the thermal stability of structural elements made of heat-resistant metals and alloys operating in a complex force and thermal field is one of the key priorities of modern high technology research. The most important case is the study of the thermal stability of structural elements in real conditions of heat fluxes with varying intensity, with a complex configuration of heat-insulated local surfaces and internal point heat sources. Many basic load-bearing structural elements operating in a large thermal field (elements of gas turbine and jet engines, etc.), are made of heat-resistant alloys. The physical feature of such alloys is that the coefficient of thermal expansion and the modulus of elasticity of the material strictly depends on the temperature distribution field, that is, the coefficients are a function of temperature. The purpose of this study is to simulate a thermo-stressed state in rod elements of a structure based on the law of conservation of energy, in the presence of a heat flux applied on the lateral surface, which varies along the coordinate in a linear manner. To solve the outlined problem, a potential energy minimisation method is used in combination of a quadratic finite element with three nodes. As a result, from the condition of the minimum of the functional defining the potential energy, a resolving system of linear algebraic equations is obtained. All possible natural boundary conditions are taken into account. In this system, all integrals used are calculated analytically. Moreover, the law of conservation of energy is fulfilled for each of the equations of the resulting system. As a result, the values of displacement, deformation and stresses were calculated, as well as the values of elastic temperature and thermoelastic components of deformations and stresses for a specific example.

Keywords: Thermal expansion, Modulus of elasticity, Thermal stress state, Displacement discretisation, Stress strain.

Corresponding Author:

Nurgul Shazhdekeyeva,
Department of Mathematics and Methods of Teaching Mathematics,
Kh. Dosmukhamedov Atyrau University,
060011, 1 Studenchesky Ave., Atyrau, Republic of Kazakhstan;
E-mail: shazhdekeyeva6526@kaiost.cn

1. Introduction

Modern internal combustion engines, gas turbine power plants, oil heating compressor stations, steam generators of nuclear reactors, and technological processes that allow the deep processing of uranium and osmium ores, as well as crude oil, pose the urgent problem of developing a mathematical model for studying the temperature distribution field of thermal, physico-mechanical state of the bearing elements of these structures, taking into account the nonlinear physical properties of materials and their operating conditions. In all technological processes, the load-bearing elements of these structures are made of heat-resistant alloys. Therefore, in the field of metallurgical science, favourable conditions are created for the production of more advanced heat-resistant alloys with high resistance to plastic deformation and fracture under the influence of high temperatures [1-15].

It is known that in a thermo-physical-mechanical process, the main characteristic that has a significant effect on the strength of load-bearing structural elements is an intense temperature rise, i.e., heat flux. In general, temperature is one of the most important characteristics of the growth process and affects the morphology and crystal structure of heat-resistant alloys. In different parts of the alloy, the distribution of the temperature field is uneven [16]. Consequently, during the thermomechanical process, in some areas of the structural elements, the temperature will be acceptable, and in some areas – critical, which leads to rapid wear of the structural elements and to the loss of their physical qualities. In this regard, for an accurate calculation of the distribution of the temperature field over the volume of multidimensional bodies of various configurations made of heat-resistant alloys, it is necessary to carry out effective theoretical and numerical modelling [17-30].

The purpose of modelling, both analytical and imitation, is to predict the state of the system, which most realistically displays the picture of the temperature field distribution over the volume of a multidimensional body. [31]. In the long term, based on this forecast, by changing both the internal parameters of the structure of structural elements and the characteristics of external influences, it will be possible to determine all the vulnerabilities in the structural elements and protect them from deformation or destruction. The development of a model of the temperature distribution over the body volume is necessary, since the complexity of the thermomechanical process in real time greatly reduces the ability to intuitively assess the identification of critical temperatures in body parts. Therefore, theoretical modelling of the temperature distribution over the volume of multidimensional bodies of various configurations made of heat-resistant alloys is undoubtedly an urgent problem.

2. Material and methods

In the case of a nonlinear one-dimensional and two-dimensional problem, the numerical simulation of the temperature distribution field in a fixed cross section is determined when the investigated temperature process depends on the applied heat flux, material length, the heat transfer coefficient, and the ambient temperature. Using all this data by the method of minimising potential energy in combination of a quadratic finite element with three nodes, the thermo-stressed state of the material is numerically assessed in the presence of a heat flux on the lateral surface, which varies along the coordinate in a linear manner.

To calculate the temperature stresses in structural elements, it is necessary to determine the temperature distribution law in the investigated elements. As known, the equation of heat conduction in a continuous medium has the form [32-45] (Eq. 1):

$$K_{xx}\frac{\partial^2 T}{\partial x^2} + K_{yy}\frac{\partial^2 T}{\partial y^2} + K_{zz}\frac{\partial^2 T}{\partial z^2} + Q = 0, \qquad (1)$$

where $T(x, y, z)$ – temperature, the dimension of which is $\cdot^\circ C$; K_{xx}, K_{yy}, K_{zz} – coefficient of thermal conductivity (of the body material) in directions x, y, z , dimensions $W/(cm \cdot^\circ C)$; Q – a heat source inside the body, which is considered positive if heat is applied to the body W/cm^3. or equation (1), the following boundary conditions hold: if the temperature is known at the points of the surface S_1 then on this surface the boundary conditions will be (Eq. 2):

$$T = T_s(S_1) \rightleftarrows \text{for } S_1, \qquad (2)$$

where T_s– set temperature at the boundary, which can be a function of the coordinates of the surface point S_1. If convective heat transfer passes through the surface S_2, which is characterised by the value $h(T - T_{OC})$, then for points of this surface the boundary conditions have the form (Eq. 3):

$$K_{xx}\frac{\partial T}{\partial x} l_x + K_{yy}\frac{\partial T}{\partial y} l_y + K_{zz}\frac{\partial T}{\partial z} l_z + h(T - T_{oc}) = 0 \text{ for } S_2 \qquad (3)$$

where h – heat transfer coefficient, $(W/(cm^2 \cdot^\circ C))$ and this coefficient can be a function of the coordinates of the points of the surface S_2; $T(x, y, z)$ – temperature at points of the surface S_2, the value of which is unknown; T_a – set temperature of the surrounding surface S_2 of the environment. It can also be a function of the coordinates of points on the surface S_2; l_x, l_y, l_z – direction cosines of surface S_2. If the heat flux q, $W/(cm \cdot {}^\circ C)$ is applied to the surface S_2 of the body, then (Eq. 4) holds for points of this surface:

$$K_{xx}\frac{\partial T}{\partial x}\ell_x + K_{yy}\frac{\partial T}{\partial y}\ell_y + K_{zz}\frac{\partial T}{\partial z}\ell_z + q = 0 \text{ for } S_3. \quad (4)$$

The given heat flux q can be a function of the coordinates of the points of the surface S_3. It should be noted here that the heat flux q and convective heat loss $h(T - T_{OC})$ do not occur on the same area of the boundary surface. This means that if there is heat loss due to convection, then there is a removal or inflow of heat due to the heat flux and vice versa. Thus, equation (1) with the reduced boundary conditions (2)-(3) has a unique solution. This solution is the law of temperature distribution in the body. But in the calculus of variations [46; 47; 48-56], it is established that solving equation (1) with boundary conditions (2)-(4) is equivalent to finding the minimum of the functional (Eq. 5):

$$J = \int_V \frac{1}{2}\left[K_{xx}\left(\frac{\partial T}{\partial x}\right)^2 + K_{yy}\left(\frac{\partial T}{\partial y}\right)^2 + K_{zz}\left(\frac{\partial T}{\partial z}\right)^2 - 2Q \cdot T\right] dV + \int_{S_2} \frac{h}{2}(T - T_{OC})^2 dS + \int_{S_3} qT dS. \quad (5)$$

In addition, equation (1) and boundary conditions (2)-(4) can be applied to one-dimensional problems by simply deleting the terms associated with unnecessary coordinates. Then the equation for the one-dimensional problem is written in the form (Eq. 6):

$$K_{xx}\frac{\partial^2 T}{\partial x^2} + Q = 0, \quad (6)$$

with the corresponding boundary conditions (Eq. 7-9):

$$T = T_3 \text{ for } S_1, \quad (7)$$

$$K_{xx}\frac{\partial T}{\partial x}\ell_x + h(T - T_{OC}) = 0 \text{ for } S_2, \quad (8)$$

$$K_{xx}\frac{\partial T}{\partial x}\ell_x + q = 0 \quad \text{for } S_3. \quad (9)$$

If there is no convective heat transfer and, in addition, the heat flux is zero, then equations (8), (9) are reduced to (Eq. 10):

$$\frac{dT}{dn} = 0, \quad (10)$$

which expresses the condition for the existence of a thermally insulated boundary. Here *n* – outward normal. In the calculus of variations, it is established that to minimise the functional (Eq. 11):

$$J = \int_V \frac{K_{xx}}{2}\left(\frac{\partial T}{\partial x}\right)^2 dV + \int_{S_2} \frac{h}{2}(T - T_{OC})^2 dS + \int_{S_3} qT dS, \quad (11)$$

it is necessary that the differential equation (6) and boundary conditions (7)-(9) are satisfied. Therefore, any temperature distribution field at which functional (11) becomes minimal also satisfies differential equations and thus is a solution to the posed problem.

3. Results and discussion

Using this statement, the thermo-stressed state of the material of the body (rod) is investigated. This study is devoted to mathematical modelling and the development of an appropriate computational algorithm for studying the thermo-stressed state of a rod clamped by two ends. On the lateral surface of the rod, a heat flux is applied, varying along the coordinate linearly [57; 58-66] (Eq. 12):

$$q(x) = ax + b, \quad (12)$$

$a, b = const$ – real numbers. In order to numerically study the thermo-physical-mechanical phenomena of the alloy material, take a rod of length $l(cm)$, the cross-sectional area $F[cm^2]$ – is constant along the length of rod. The physical and mechanical properties of the rod material are characterised by the modulus of elasticity $E\left[\frac{kg}{cm^2}\right]$, the coefficient of thermal expansion $\alpha\left(\frac{1}{°C}\right)$, heat exchange with the environment $h\left[\frac{W}{cm^2 \cdot °C}\right]$ and thermal conductivity$K_{xx}\left(\frac{W}{cm^2 \cdot °C}\right)$. Through the cross-sectional areas of the two clamped ends, heat exchange of different intensities occurs with the media surrounding them. The heat transfer coefficient for the left end of the rod is denoted by $h_0[\frac{W}{(cm^2 \cdot °C)}]$, and the temperature of the environment surrounding this area – $T_{oc}(°C)$, and for the right end, respectively – $h_1[\frac{W}{(cm^2 \cdot °C)}]$ and $T_{ocl}(°C)$. The diagram scheme for this problem is presented in Figure 1.

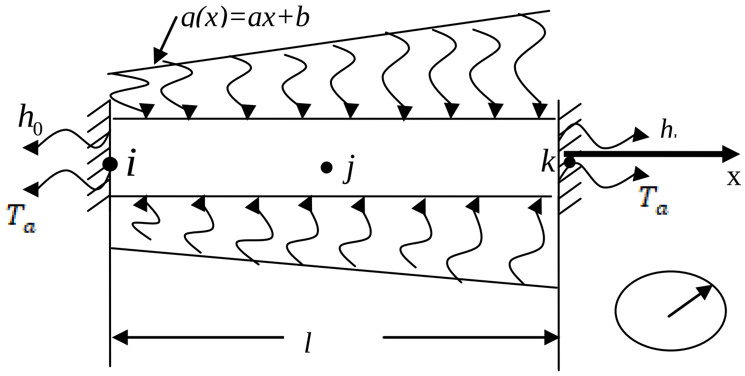

F= πr^2 – cross-sectional area
$P = 2\pi r$ – cross-sectional perimeter

Figure 1. Analytical model

The rod heats up due to the action on the lateral surface of a given heat flux $q(x)(\frac{W}{cm^2})$. In this regard, it is expanding. Since both ends of the rod are rigidly restrained, it cannot be lengthened. In this regard, a compressive force $R(kg(f))$, arises at the two ends of the rod, which leads to the appearance of a stress $\sigma, (kg(f)/cm^2)$ in the sections of the rod. Such a task is called statically indeterminate. Despite this, this problem can be solved numerically if the potential energy minimisation method is used in combination with a quadratic finite element with three nodes. The equation of potential energy for the considered problem is defined as follows [67; 68; 69-80] (Eq. 13):

$$\Pi = \int_V \frac{\sigma_x \cdot \varepsilon_x}{2} dv - \int_V \alpha \cdot E \cdot T(X) \cdot \varepsilon_x dv, \tag{13}$$

where V, (cm^3) – volume of the considered bearing rod element; *u*(*x*), (cm) – displacement distribution field of the cross section of the rod; field distribution of elastic component of deformation (longitudinal deformation) (Eq. 14)

$$\varepsilon_x = \frac{\partial u}{\partial x}; \tag{14}$$

the field of distribution of the elastic component of the compression-tension stress (Eq. 15-16);

$$\sigma_x = E, \tag{15}$$

$$\varepsilon_x = E \cdot \frac{\partial u}{\partial x}(kg(f)/cm^2); \tag{16}$$

field distribution of the elasticity modulus of the material of the rod element (17):

$$E = E(T(x)) \tag{17}$$

and $\alpha(T(x))$ – field of distribution of the coefficient of thermal expansion of the material of the rod element, which depend on temperature; temperature distribution law along the length of the bearing element (Eq. 18):

$$T = T(x), \tag{18}$$

which is approximated by a complete second-order polynomial, i.e., [81; 82; 83; 84-102] (Eq. 19):

$$T(x) = ax^2 + bx + c; \text{ at } 0 \leq x \leq l \,, \tag{19}$$

where a, b, c – some constants whose values are still unknown. To find the value of these constants, divide the considered part of the rod in half. And in this part three nodes (i, j, k) are fixed (Figure 2).

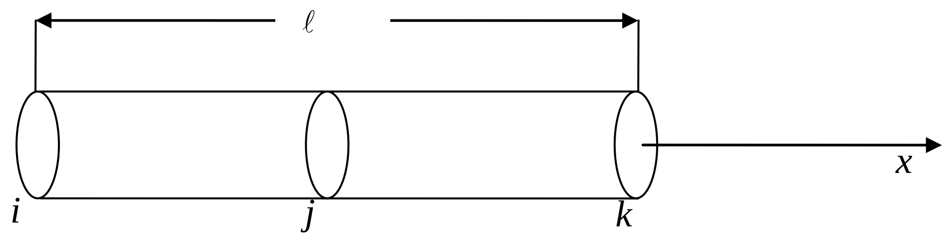

Figure 2. One-dimensional quadratic finite element

The global coordinates of these nodes are respectively x_i, x_j, x_k, while (Eq. 20):

$$x_j = \frac{x_i + x_k}{2}. \tag{20}$$

In this case, in the local system, the coordinates of the three nodes are determined as follows (Eq. 21-23):

$$x_i = 0; \tag{21}$$

$$x_j = \frac{\ell}{2}; \tag{22}$$

$$x_k = \ell. \tag{23}$$

Next, introduce the following notation characterising the temperature value at nodesi, j, k (Eq. 24):

$$T_i = T(x = x_i); \quad T_j = T(x = x_j); \quad T_k = T(x = x_k). \tag{24}$$

Then, substituting (24) into (19), a system of three equations is composed to determine the values of the constants a, b, c (Eq. 25):

$$\left.\begin{aligned} ax_i^2 + bx_i + c = T_i; \\ ax_j^2 + bx_j + c = T_j; \\ ax_k^2 + bx_k + c = T_k; \end{aligned}\right\} \tag{25}$$

taking into account that (21)-(23), from the last system obtain (Eq. 26):

$$\left.\begin{aligned} & c = T_i; \\ & \frac{\ell^2}{4}a + \frac{\ell}{2}b + c = T_j; \\ & \ell^2 a + \ell b + c = T_k. \end{aligned}\right\} \tag{26}$$

Considering that (Eq. 27):

$$c = T_i, \tag{27}$$

from the last two equations of system (26) obtain (28):

$$\left.\begin{aligned} \frac{\ell^2}{4}a + \frac{\ell}{2}b = T_j - T_i; \\ \ell^2 a + \ell b = T_k - T_i. \end{aligned}\right\} \tag{28}$$

From here it follows (Eq. 29):

$$\left.\begin{aligned} a &= \frac{2(T_k - 2T_j + T_i)}{\ell^2}; \\ b &= \frac{4T_j - T_k - 3T_i}{\ell}; \\ c &= T_i. \end{aligned}\right\} \tag{29}$$

Substituting the obtained values of a, b, c into (19), obtain (Eq. 30):

$$T(x) = \frac{(2T_k - 4T_j + 2T_i)}{\ell^2}x^2 + \frac{(4T_j - T_k - 3T_i)}{\ell}x + T_i = \frac{\ell^2 - 3\ell x + 2x^2}{\ell^2}T_i + \frac{4\ell x - 4x^2}{\ell^2}T_j + \frac{2x^2 - \ell x}{\ell^2}T_k \tag{30}$$

Let us introduce the following equation (31):

$$\left.\begin{aligned} \phi_i(x) &= \frac{\ell^2 - 3\ell x + 2x^2}{\ell^2}; \\ \phi_j(x) &= \frac{4\ell x - 4x^2}{\ell^2}; \\ \phi_k(x) &= \frac{2x^2 - \ell x}{\ell^2}. \end{aligned}\right\} \tag{31}$$

Then, taking into account (31), rewrite (30) in the following form (32):

$$T(x) = \phi_i(x)T_i + \phi_j(x)T_j + \phi_k(x)T_k, \text{ at } 0 \le x \le \ell, \tag{32}$$

where the functions $\phi_i(x)$, $\phi_j(x)$, $\phi_k(x)$ are called form functions for a one-dimensional quadratic finite element with three nodes. It should be noted that these form functions have certain properties. Now consider the properties of these form functions (Eq. 33-34):

$$\left.\begin{aligned} \phi_i(x)|_{x=x_i} = \phi_i(x = x_i = 0) = 1; \\ \phi_j(x)\big|_{x=x_i} = \phi_j(x = x_i = 0) = 0; \\ \phi_k(x)|_{x=x_i} = \phi_k(x = x_i = 0) = 0. \end{aligned}\right\}, \tag{33}$$

$$\left.\begin{aligned} \phi_i(x)|_{x=x_j} = \phi_i(x = x_j = \tfrac{\ell}{2}) = 0; \\ \phi_j(x)\big|_{x=x_j} = \phi_j(x = x_j = \tfrac{\ell}{2}) = 1; \\ \phi_k(x)|_{x=x_j} = \phi_k(x = x_j = \tfrac{\ell}{2}) = 0. \end{aligned}\right\}, \tag{34}$$

$$\left.\begin{aligned} \phi_i(x)|_{x=x_k} = \phi_i(x = \ell) = 0; \\ \phi_j(x)\big|_{x=x_k} = \phi_j(x = \ell) = 0; \\ \phi_k(x)|_{x=x_k} = \phi_k(x = \ell) = 1. \end{aligned}\right\}, \tag{35}$$

In addition, for any point of (Eq. 36):

$$x = x_\phi \tag{36}$$

in the range $0 \le x \le \ell$ one has (Eq. 37):

$$\phi_i(x_\phi) + \phi_j(x_\phi) + \phi_k(x_\phi) = 1. \tag{37}$$

For example (Eq. 38):

$$x_\phi = \frac{\ell}{4}. \tag{38}$$

Then (Eq. 39):

$$\phi_i(x_\phi) + \phi_j(x_\phi) + \phi_k(x_\phi) = \frac{\ell^2 - 3\ell\frac{\ell}{4} + 2\frac{\ell^2}{16}}{\ell^2} + \frac{4\ell\frac{\ell}{4} - 4\frac{\ell^2}{16}}{\ell^2} + \frac{2\frac{\ell^2}{16} - \ell\frac{\ell}{4}}{\ell^2} = \frac{3}{8} + \frac{3}{4} - \frac{1}{8} = \frac{3+6-1}{8} = 1 \tag{39}$$

Also, form functions have the following properties. For any point of the interval $0 \le x \le \ell$, i.e., within each finite element one has (Eq. 40):

$$\frac{\partial \phi_i(x)}{\partial x} + \frac{\partial \phi_j(x)}{\partial x} + \frac{\partial \phi_k(x)}{\partial x} = 0. \tag{40}$$

Using equation (31), prove (Eq. 41):

$$\left.\begin{aligned} \frac{\partial \phi_i(x)}{\partial x} &= \frac{1}{\ell^2}(-3\ell + 4x); \\ \frac{\partial \phi_j(x)}{\partial x} &= \frac{4}{\ell^2}(\ell - 2x); \\ \frac{\partial \phi_k(x)}{\partial x} &= \frac{1}{\ell^2}(4x - \ell). \end{aligned}\right\}. \tag{41}$$

Next, find the total (Eq. 42):

$$\frac{\partial \phi_i(x)}{\partial x} + \frac{\partial \phi_j(x)}{\partial x} + \frac{\partial \phi_k(x)}{\partial x} = \frac{1}{\ell^2}[-3\ell + 4x + 4\ell - 8x + 4x - \ell] = 0. \tag{42}$$

Within the length of the element under consideration, the displacement distribution field (Eq. 43):

$$u = u(x), \tag{43}$$

approximating by a second-order polynomial, obtain (Eq. 44):

$$u = u(x) = \varphi_i(x) \cdot u_i + \varphi_j(u_j) + \varphi_k(x) \cdot u_k, \tag{44}$$

where u_i, u_j, u_k – displacements of the section of the rod, the coordinates of which (Eq. 45):

$$x = 0;\ x = \frac{l}{2};\ x = l. \tag{45}$$

Then, within the limits of the length of the rod (the element under consideration), the displacement gradient, i.e., the distribution field of the elastic component of deformation (ε_x) is expressed as follows (Eq. 46):

$$\varepsilon_x = \frac{\partial u}{\partial x} = \frac{\partial \varphi_i(x)}{\partial x} u_i + \frac{\partial \varphi_j(x)}{\partial x} u_j + \frac{\partial \varphi_k(x)}{\partial x} u_k. \tag{46}$$

Based on Hooke's law, the value of the elastic stress component is determined as follows (Eq. 47):

$$\sigma_x = E \cdot \varepsilon_x = E \cdot \left(\frac{4x - 3l}{l^2} u_i + \frac{4l - 8x}{l^2} u_j + \frac{4x - l}{l^2} u_k \right) \tag{47}$$

According to the theory of thermoelasticity, the values of deformation from the temperature field are determined by the equation (Eq. 48):

$$\varepsilon_T = -\alpha T(x). \tag{48}$$

The values of the temperature component of the voltage are determined by the equation (Eq. 49):

$$\sigma_T = E \cdot \varepsilon_T\,, \tag{49}$$

a of thermoelastic stress (Eq. 50):

$$\sigma = \sigma_x + \sigma_T. \tag{50}$$

The cross-sectional area of the rod $F(cm^2)$ is constant along the length, equation (13) is written in the following form (Eq. 51):

$$\Pi = \int\limits_V \frac{\sigma_x}{2} \cdot \varepsilon_x \cdot dv - \int\limits_V \alpha \cdot E \cdot T(x) \cdot \varepsilon_x \cdot dv =$$

$$= \frac{F}{2}\int\limits_0^l \sigma_x \cdot \varepsilon_x dx - F \cdot \int\limits_o^l \alpha \cdot E \cdot T(x) \cdot \varepsilon_x \cdot dx =$$

$$= \frac{E \cdot F}{2}\int_0^l \varepsilon_x^2 \cdot dx - \alpha \cdot E \cdot F \cdot \int_0^l T(x) \cdot \varepsilon_x \cdot dx\,; \tag{51}$$

In order to improve the accuracy and improve the convergence of the obtained numerical results, two intergrades are analytically integrated in volume (52):

$$\Pi = \frac{E}{2}\int_V \varepsilon_x^2 dV - \alpha E\int_V T(x)\varepsilon_x dV = \frac{EF}{2}\int_0^\ell \varepsilon_x^2 dx - \alpha EF\int_0^\ell T(x)\varepsilon_x\, dx =$$

$$= \frac{EF}{2\ell^4}\left\{\left[\frac{16x^3}{3} - 12\ell x^2 + 9\ell^2 x\right]u_i^2 + 2\left[20\ell x^2 - \frac{32x^3}{3} - 12\ell^2 x\right]u_i u_j + 2\left[\frac{16x^3}{3} - 8\ell x^2 + 3\ell^2 x\right]u_i u_k + \right.$$

$$\left.+\left[16\ell^2 x - 32\ell x^2 - \frac{64x^3}{3}\right]u_j^2 + 2\left[12\ell x^2 - \frac{32x^3}{3} - 4\ell^2 x\right]u_j u_k + \left[\frac{16x^3}{3} - 4\ell x^2 + \ell^2 x\right]u_k^2\right\}\Bigg|_0^\ell -$$

$$-\frac{\alpha EF}{\ell^4}\left\{\left[\frac{13\ell^2 x^2}{2} - 6\ell x^3 - 3\ell^3 x + 2x^4\right]T_i u_i + \left[\frac{32\ell x^3}{3} - 10\ell^2 x^2 + 4\ell^3 x - 4x^4\right]T_i u_j + \right.$$

$$+\left[\frac{7\ell^2 x^2}{2} - \frac{14\ell x^3}{3} - \ell^3 x + 2x^4\right]T_i u_k + \left[\frac{28\ell x^3}{3} - 6\ell^2 x^2 + 4x^4\right]T_j u_i + [8\ell^2 x^2 - 16\ell x^3 + 8x^4]T_j u_j +$$

$$+\left[\frac{20\ell x^3}{3} - 2\ell^2 x^2 - 4x^4\right]T_j u_k + \left[\frac{32\ell^2 x^2}{2} - \frac{10\ell x^3}{3} + 2x^4\right]T_k u_i + \left[\frac{16\ell x^3}{3} - 2\ell^2 x^2 - 4x^4\right]T_k u_j +$$

$$\left.+\left[\frac{\ell^2 x^2}{2} - 2\ell x^3 + 2x^4\right]T_k u_k\right\}\Bigg|_0^\ell = \frac{EF}{6\ell}\left[7u_i^2 - 16u_i u_j + 2u_i u_k + 16u_j^2 - 16u_j u_k + 7u_k^2\right] -$$

$$-\frac{\alpha EF}{6}\left[-3T_i u_i + 4T_i u_j - T_i u_k - 4T_j u_i + 4T_j u_k + T_k u_i - 4T_k u_j + 3T_k u_k\right] \tag{52}$$

It should be noted here that the total of the coefficients in square brackets is zero. This shows the convergence of the obtained numerical results. Using the obtained calculations in equation (52), it is possible to write the final integrated form of the potential energy formula (Eq. 53):

$$\Pi = \frac{EF}{6l}\left[7u_i^2 - 16u_iu_j + 2u_iu_k + 16u_j^2 - 16u_ju_k + 7u_k^2\right] -$$

$$-\frac{\alpha\cdot E\cdot F}{6}\left[-3T_iu_i + 4T_iu_j - T_iu_k - 4T_ju_i + 4T_ju_k + T_ku_i - 4T_ku_j + +3T_ku_k\right] \quad (53)$$

Considering that the nodal temperature values are known, the potential energy will be minimised by the nodal displacement values. As a result, obtain a system of linear algebraic equations (Eq. 54):

$$1)\ \frac{\partial \Pi}{\partial u_i} = 0 \Longrightarrow \frac{7EF}{3l}u_i - \frac{8EF}{3l}u_j + \frac{EF}{3l}u_k = -\frac{\alpha EF}{2}T_i - \frac{2\alpha EF}{3}T_j + \frac{\alpha EF}{6}T_k;$$

$$2)\ \frac{\partial \Pi}{\partial u_j} = 0 \Longrightarrow -\frac{8EF}{3l}u_i + \frac{16EF}{3l}u_j - \frac{8EF}{3l}u_k = \frac{2\alpha EF}{3}T_i - \frac{2\alpha EF}{3}T_k;$$

$$3)\ \frac{\partial \Pi}{\partial u_k} = 0 \Longrightarrow \frac{EF}{3l}u_i - \frac{8EF}{3l}u_j + \frac{7EF}{3l}u_k = -\frac{\alpha EF}{6}T_i + \frac{2\alpha EF}{3}T_j + \frac{\alpha EF}{2}T_k. \quad (54)$$

To test the developed computational algorithm, the following test problem is taken [103-124]: rod length – $l = 30cm.$, radius of the cross-section of the rod $-r = 2\,cm$, constant along the length of the rod, the elasticity modulus of the rod material – $E = 2\cdot 10^6\,kg/cm^2$, coefficient of thermal expansion $\alpha = 125\cdot 10^{-7}(1/°C)$, coefficient of thermal conductivity of the rod material – $K_{xx} = 72(W/(cm°C))$. Heat flux – $q(x) = -[3x + 10]\ (W/cm^2)$ is applied to the lateral surface of the rod by a linear law. Solving the system of linear algebraic equations (38) with the accepted initial data and using the property of the applied quadratic finite element, calculate the values of displacement, deformation, and stress for different (N=1) – one quadratic finite element (QFE), N=2-QFE, N=3-QFE, N=5-QFE, N=10-QFE), i.e., at 11, at 20, at 30, at 50, at a 100 equally spaced points and ten intervals between them. All calculated values and displacements, $\varepsilon_x, \varepsilon_T, \varepsilon_u, \sigma_x, \sigma_T, \sigma_u$ – elastic, temperature, and thermoelastic components of deformations and stresses were given in the corresponding tables (Table 1).

Table 1. Values and displacements, $\varepsilon_x, \varepsilon_T, \varepsilon_u, \sigma_x, \sigma_T, \sigma_u$ – elastic, temperature, and thermoelastic components of deformations and stresses

Nodal points	ε_x	Nodal points	ε_T	Nodal points	ε_u
1	-0.0007335304	1	-0.0015142235	1	-0.0022477539
3	-0.0001168919	3	-0.0021320339	3	-0.0022489258
4	0.0001211149	4	-0.0023717985	4	-0.0022506836
7	0.0003945101	7	-0.0026457797	7	-0.0022512695
9	0.0000642736	9	-0.0023167151	9	-0.0022524414
10	-0.0002977196	10	-0.0019564796	10	-0.0022541992
Total:					-0.0225097656
Nodal points	σ_x	Nodal points	σ_T	Nodal points	σ_u
1	-1467.0608108108	1	-3028.4470016892	1	-4495.5078125000
3	-233.7837837838	3	-3682.9761402027	3	-4497.8515625000
4	242.2297297297	4	-4743.5969172297	4	-4501.3671875000
7	789.0202702703	7	-5291.5593327703	7	-4502.5390625000
9	128.5472972973	9	-4633.4301097973	9	-4504.8828125000
10	-595.4391891892	10	-5083.5884712838	10	-4508.3984375000

Arithmetic mean:	-4501.9531250000

Note: $\sigma_u = -4501.953125$.

The values of 11 nodal displacements and the corresponding law of distribution of deformation and stress are presented in Figures 3-4:

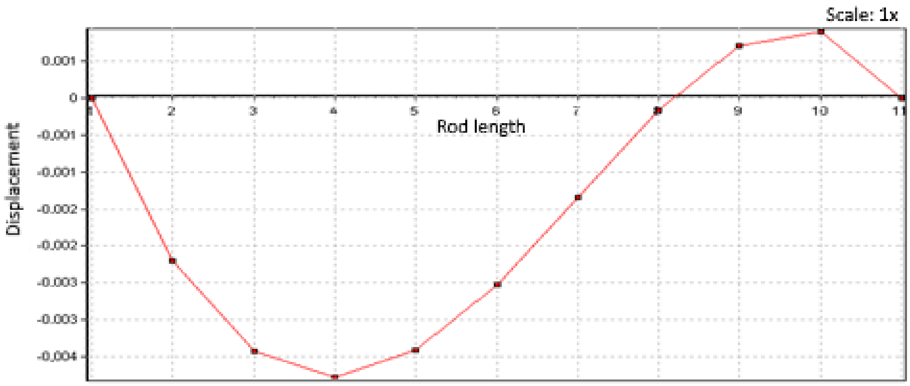

Figure 3. Values of 11 nodal displacements along the length of the rod

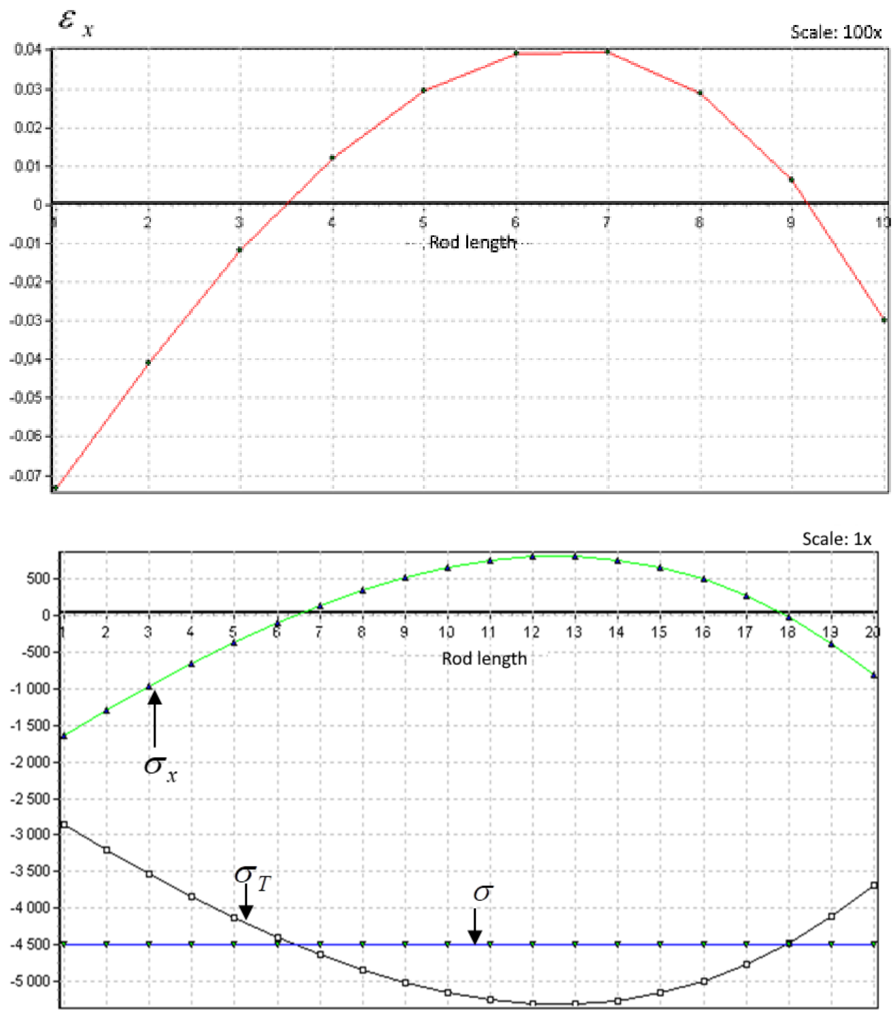

Figure 4. Fields of distribution of the value of 11 nodal displacements corresponding to deformation and stress (ε_x, σ_x, σ_T, σ) along the length of the rod

Similarly, the distribution field of the deformation value from the temperature field ε_T is presented in Figure 5

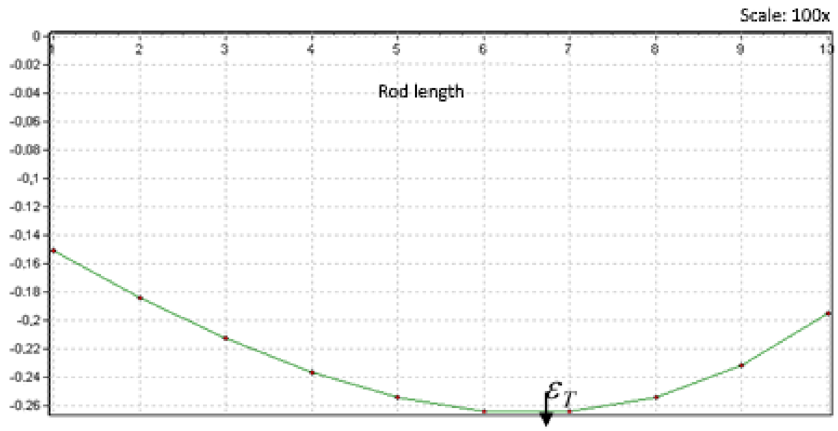

Figure 5. Values of 11 nodal deformations from the temperature field ε_T along the length of the rod

Analysing Table 1, it can be seen that the value of thermoelastic stress exceeds the exact ($\sigma = -4494.79\ kg(f)/cm^2$) solution by a maximum of 0.16%. In this regard, the considered rod is discretised with two (N=2) quadratic finite elements. At twenty fixed points, the values of elastic, temperature and thermoelastic components of deformations and stresses – ε_x, ε_T, ε_u, σ_x, σ_T, σ_u are given in Table 2, the corresponding fields of displacement, deformation and stress distribution in Figures 6-7, and the distribution field ε_T in the Figure 8.

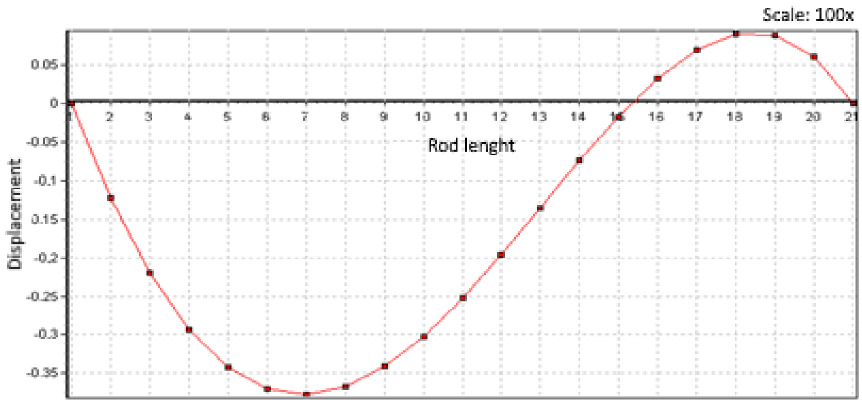

Figure 6. Values of 20 nodal displacements along the length of the rod

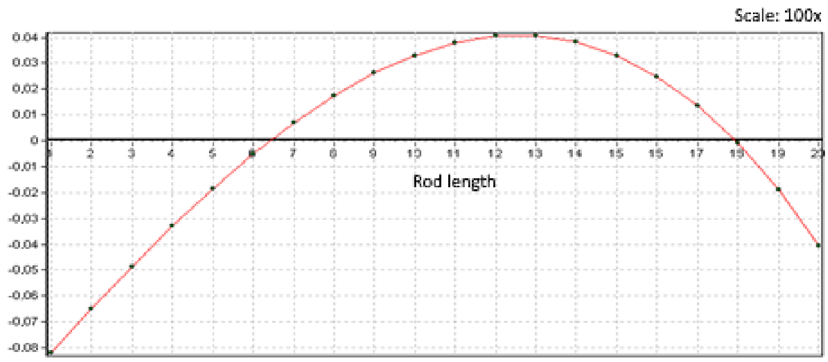

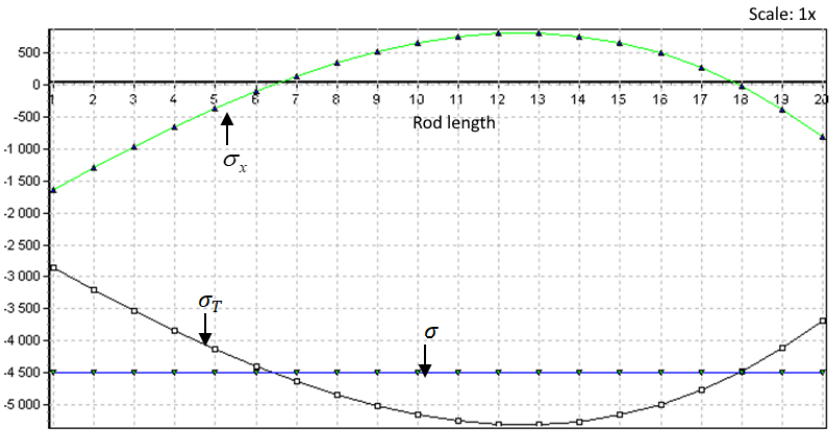

Figure 7. Fields of distribution of the value of 20 nodal values corresponding to deformation and stress (ε_x, σ_x, σ_T, σ) along the length of the rod

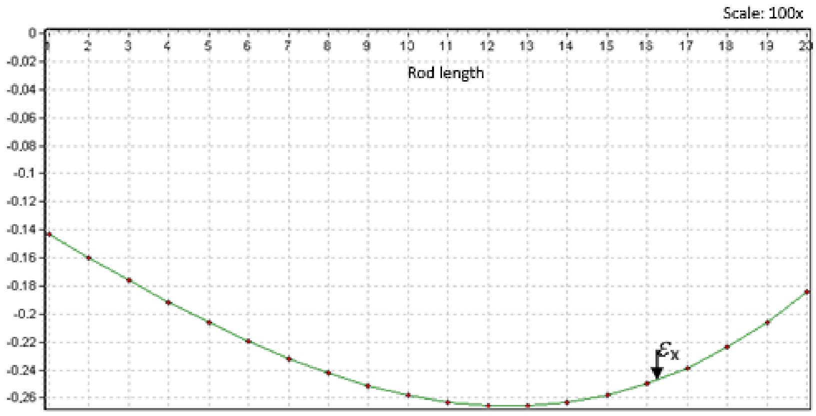

Figure 8. Values of 20 nodal deformations from the temperature field ε_T along the length of the rod

Table 2. Values of elastic, temperature, and thermoelastic components of deformations and stresses

Nodal points	ε_x	Nodal points	ε_T	Nodal points	ε_u
1	-0.0008192040	1	-0.0014283180	1	-0.0022475220
6	-0.0000507496	6	-0.0021972851	6	-0.0022480347
7	0.0000694257	7	-0.0023173871	7	-0.0022479614
13	0.0004061022	13	-0.0026545031	13	-0.0022484009
17	0.0001364126	17	-0.0023851064	17	-0.0022486938
20	-0.0004054054	20	-0.0018436547	20	-0.0022490601
Total:					-0.0449658203
Nodal points	σ_x	Nodal points	σ_T	Nodal points	σ_u
1	-1638.4079391892	1	-2856.6360061233	1	-4495.0439453125
6	-101.4991554054	6	-4394.5701805321	6	-4496.0693359375
7	138.8513513514	7	-4634.7742029138	7	-4495.9228515625
13	812.2043918919	13	-5309.0061497044	13	-4496.8017578125
17	272.8251689189	17	-4770.2128642314	17	-4497.3876953125
18	-18.0743243243	18	-4479.7528241131	18	-4497.8271484375

20	-810.8108108108	20	-3687.3093063767	20	-4498.1201171875
Arithmetic mean:					-4496.5820312500

Note: $\sigma_u = -4496.58$.

Analysing Table 2, it can be seen that the largest deviation from the exact ($\sigma = -4494.79\ kg(f)/cm^2$) solution is 0.04%. For engineering calculations, this accuracy is considered to be excellent, but, nevertheless, in order to reduce the error of the obtained numerical results, the considered rod is discretised with three (N=3) quadratic finite elements of the same length. As a result of solving the resolving systems of equations, the values of the sought variables at thirty fixed points are obtained and presented in Table 3, and the corresponding displacement field and the law of distribution of elastic, temperature, and thermoelastic components of deformations and stresses (ε_x, σ_x, σ_T, σ) along the length of the rod are given in Figures 9 -10, and the law of deformation distribution from the temperature field (ε_T) is given in Figure 11:

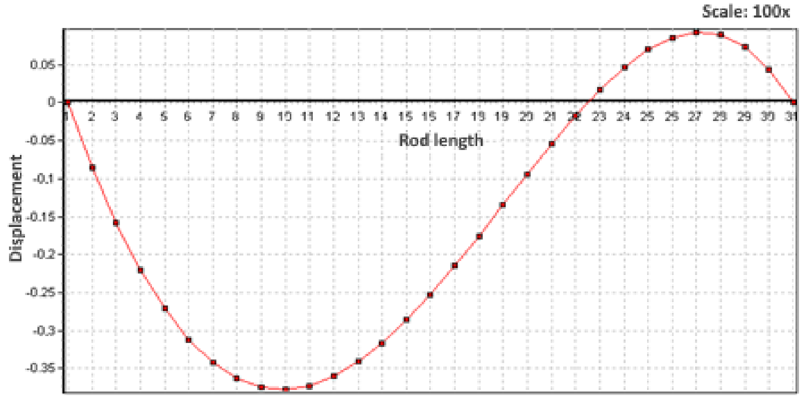

Figure 9. Values of 30 nodal displacements along the length of the rod

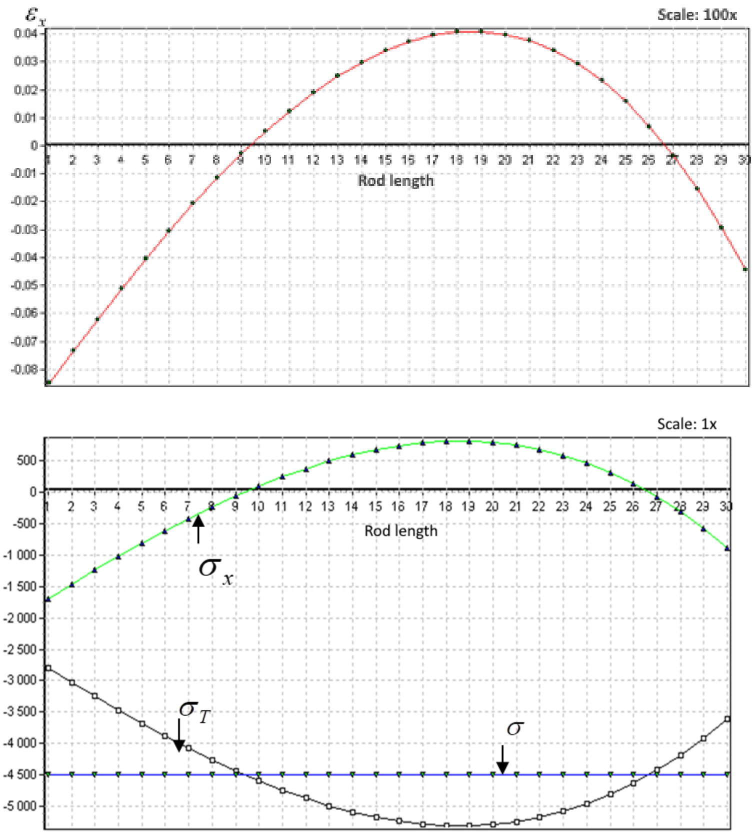

Figure 10. Fields of distribution of 30 nodal values corresponding to deformation and stress (ε_x, σ_x, σ_T, σ) along the length of the rod

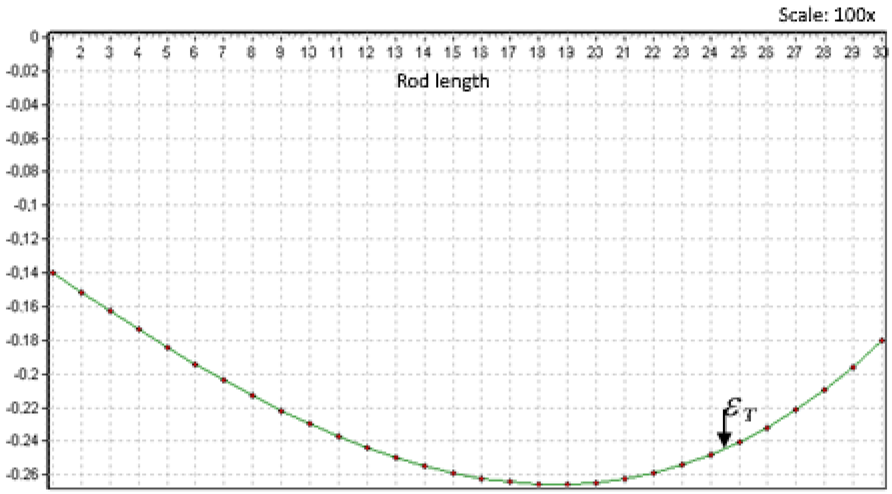

Figure 11. Fields of distribution of values of 30 nodal deformations from the temperature field ε_T along the length of the rod

Table 3. The values of the sought variables at 30 fixed points

Nodal points	ε_x	Nodal points	ε_T	Nodal points	ε_u
1	-0.0008480512	1	-0.0013994061	1	-0.0022474573
9	-0.0000293387	9	-0.0022182922	9	-0.0022476309
10	0.0000506913	10	-0.0022983874	10	-0.0022476960
19	0.0004081144	19	-0.0026559623	19	-0.0022478479
26	0.0000686718	26	-0.0023167151	26	-0.0022480433
27	-0.0000356732	27	-0.0022123484	27	-0.0022480216
30	-0.0004441942	30	-0.0018039359	30	-0.0022481301
				Total:	-0.0674338108
Nodal points	σ_x	Nodal points	σ_T	Nodal points	σ_u
1	-1696.1023523523	1	-2798.8122888512	1	-4494.9146412035
9	-58.6774274274	9	-4436.5844359983	9	-4495.2618634257
10	101.3826326326	10	-4596.7747043917	10	-4495.3920717591
19	816.2287287287	19	-5311.9246199322	19	-4495.6958912035
26	137.3435935936	26	-4633.4301097971	26	-4496.0865162035
27	-71.3463463463	27	-4424.6967670794	27	-4496.0431134257
30	-888.3883883883	30	-3607.8717389263	30	-4496.2601273146
Arithmetic mean:					-4495.5873842591

Note: $\sigma_u = -4495.58$.

In this case, it was revealed from the obtained numerical solutions that the maximum discrepancy between the σ_u value and the exact one $(\sigma_u = -4494.79\ kg(f)/cm^2)$ is 0.017576%. Thus, it was found that with an increase in discrete finite elements, a decrease in errors is observed. If the considered rod is discretised with five (N=5) quadratic finite elements, then the obtained numerical results in Table 4 show that the maximum error in the value of the thermoelastic stress does not exceed 0.00641%.

Table 4. Numerical results of discretising a rod by five quadratic finite elements

Nodal points	ε_x	Nodal points	ε_T	Nodal points	ε_u
1	-0.0008712331	1	-0.0013761864	1	-0.0022474195
15	-0.0000126642	15	-0.0022348210	15	-0.0022474852
16	0.0000353872	16	-0.0022828864	16	-0.0022474992
31	0.0004090574	31	-0.0026566176	31	-0.0022475602
44	0.0000083000	44	-0.0022559305	44	-0.0022476305
45	-0.0000579986	45	-0.0021896271	45	-0.0022476258
50	-0.0004762669	50	-0.0017713917	50	-0.0022476586
Total:					-0.1123769531
Nodal points	σ_x	Nodal points	σ_T	Nodal points	σ_u
1	-1742.4662162164	1	-2752.3728462840	1	-4494.8390625
15	-25.3283783784	15	-4469.6419341219	15	-4494.9703125
16	70.7743243243	16	-4565.7727618247	16	-4494.9984375
31	818.1148648650	31	-5313.2351773653	31	-4495.1203125
44	16.6000000000	44	-4511.8609375003	44	-4495.2609375
45	-115.9972972973	45	-4379.2542652030	45	-4495.2515625
50	-952.5337837839	50	-3542.7834037165	50	-4495.3171875
Arithmetic mean:					-4495.0781250004

Note: $\sigma_u = -4495.0781$.

The corresponding field of distribution of displacements along the length of the rod is presented in Figure 12.

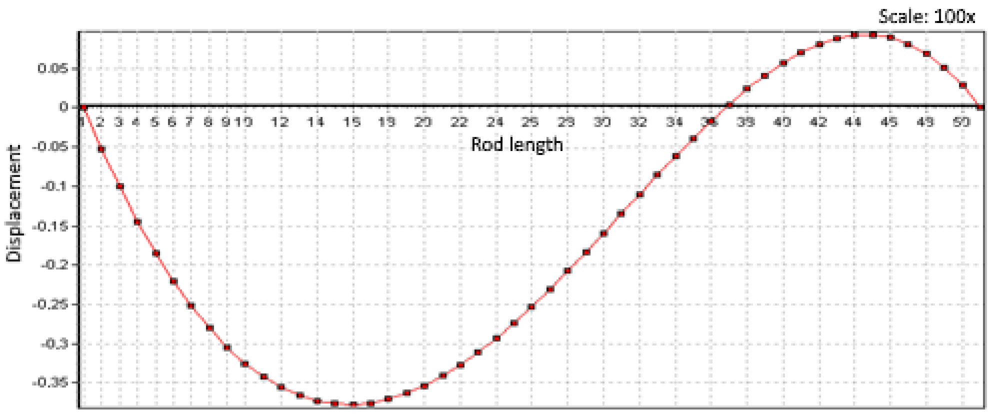

Figure 12. Values of 50 nodal displacements along the length of the rod

This curve is based on the displacement values at 51 equidistant points. In this case, the distance between the points is 0.6 cm. It can be seen from this graph that approximately at the point with the coordinate $x = 21.6\,cm$ the displacement value will be zero. The corresponding strain and stress fields are presented in Figures 13-14.

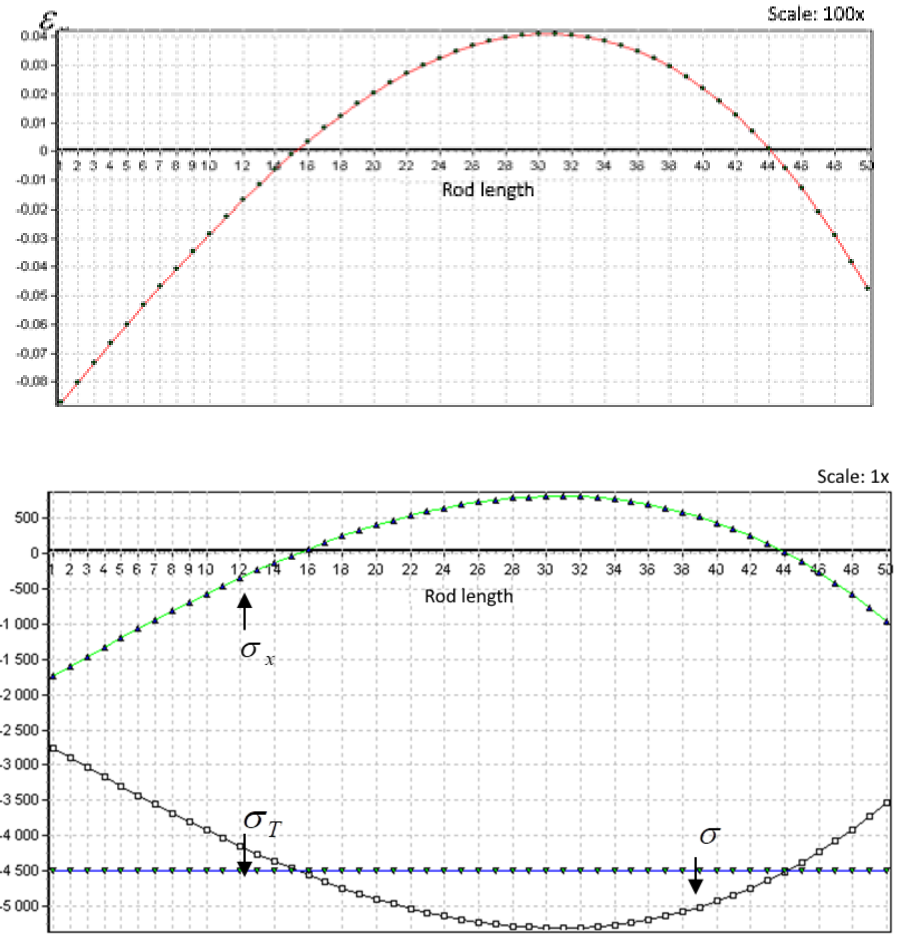

Figure 13. Fields of distribution of 50 nodal values corresponding to deformation and stress (ε_x, σ_x, σ_T, σ) along the length of the rod

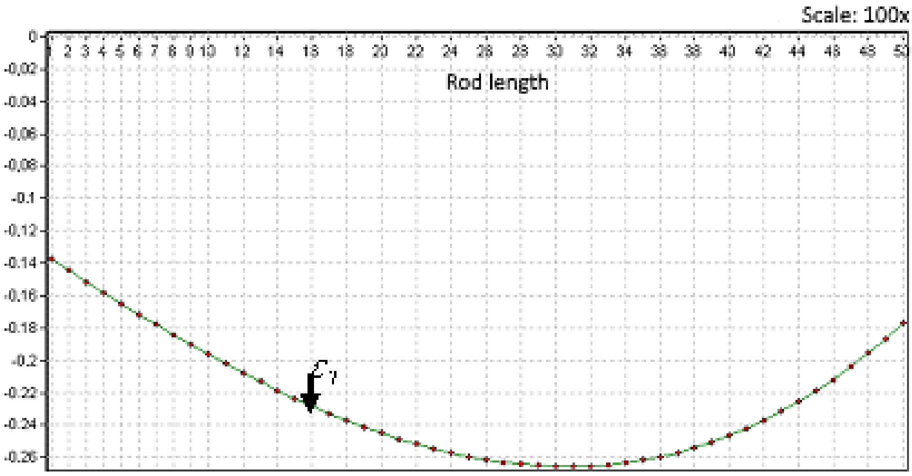

Figure 14. Fields of distribution of the value of 50 nodal deformations from the temperature field ε_T along the length of the rod

Then discretise the considered rod with ten (N=10) quadratic finite elements, then the obtained numerical value of the thermoelastic stress in Table 5 exceeds the exact ($\sigma_u = -4494.79\ kg(f)/cm^2$) solution by 0.00163%.

Table 5. Numerical value of thermoelastic stress

Nodal points	ε_x	Nodal points	ε_T	Nodal points	ε_u
1	-0.0008886803	1	-0.0013587217	1	-0.0022474021
30	-0.0000003670	30	-0.0022470532	30	-0.0022474202
31	0.0000236681	31	-0.0022710877	31	-0.0022474196
61	0.0004093758	61	-0.0026568131	61	-0.0022474372
87	0.0000241872	87	-0.0022716396	87	-0.0022474524
88	-0.0000075778	88	-0.0022398764	88	-0.0022474542
100	-0.0005009291	100	-0.0017465322	100	-0.0022474612
Total:					-0.2247431641
Nodal points	σ_x	Nodal points	σ_T	Nodal points	σ_u
1	-1777.3606418924	1	-2717.4434596715	1	-4494.8041015639
30	-0.7339527025	30	-4494.1064769865	30	-4494.8404296890
31	47.3361486489	31	-4542.1754064628	31	-4494.8392578140
61	818.7516891894	61	-5313.6261032534	61	-4494.8744140640
87	48.3743243241	87	-4543.2792071381	87	-4494.9048828140
88	-15.1555743246	88	-4479.7528241144	88	-4494.9083984390
100	-1001.8581081080	100	-3493.0643528303	100	-4494.9224609390
Arithmetic mean:					-4494.8632812515

Note: $\sigma_u = -4494.86328$.

This accuracy in terms of thermal stability is very excellent. In this case, the corresponding field of displacement distribution is presented in Figure 15:

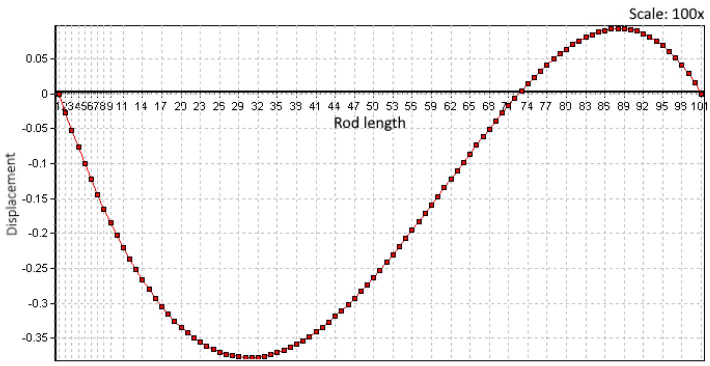

Figure 15. Values of 100 nodal displacements along the length of the rod

This figure shows that near the point $x = 21.6$ cm the displacement value will again be zero. The constructed deformation and stress fields are presented in Figures 16-17.

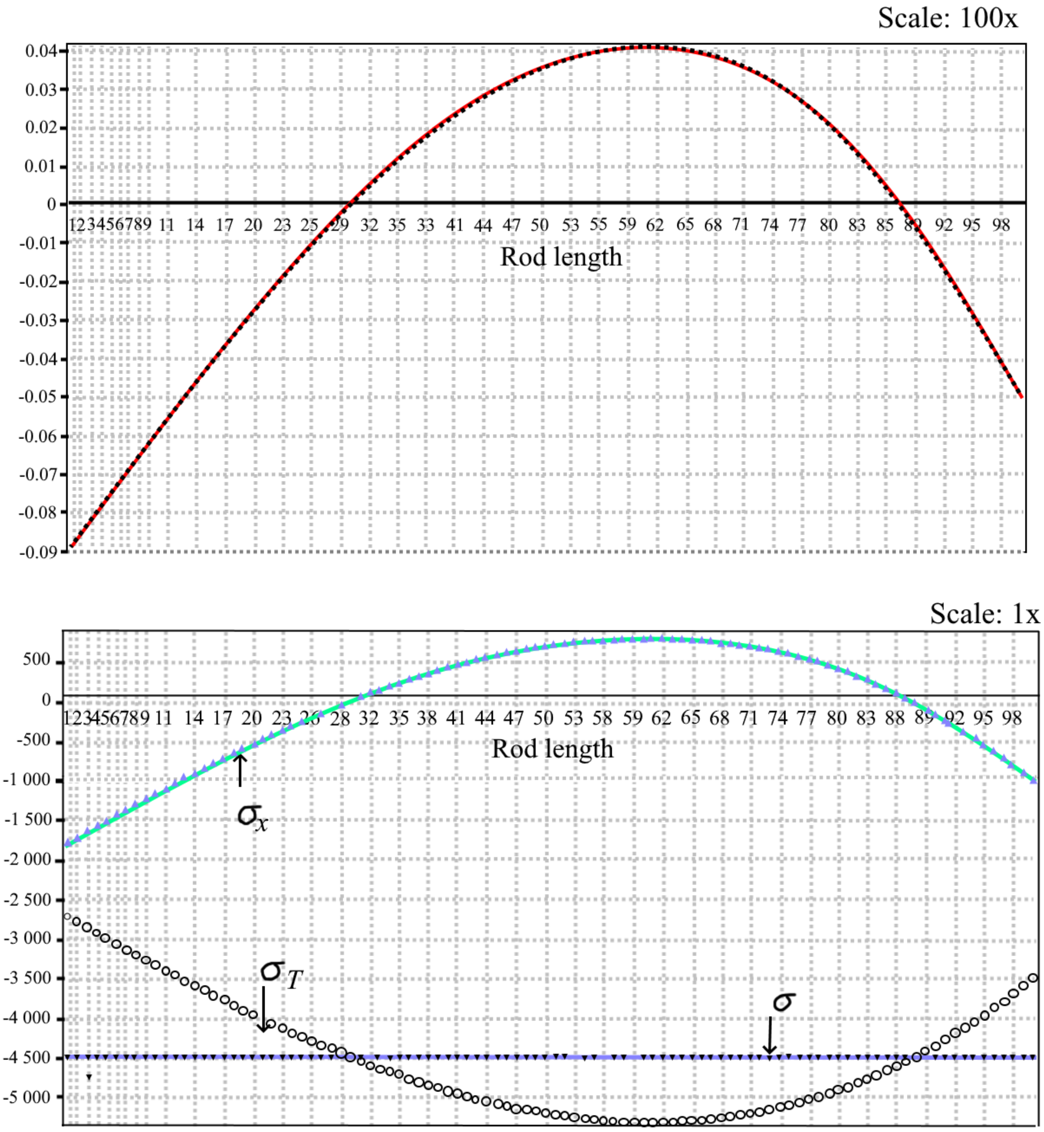

Figure 16. Fields of distribution of the value of 100 nodal displacements corresponding to deformation and stress (ε_x, σ_x, σ_T, σ) along the length of the rod

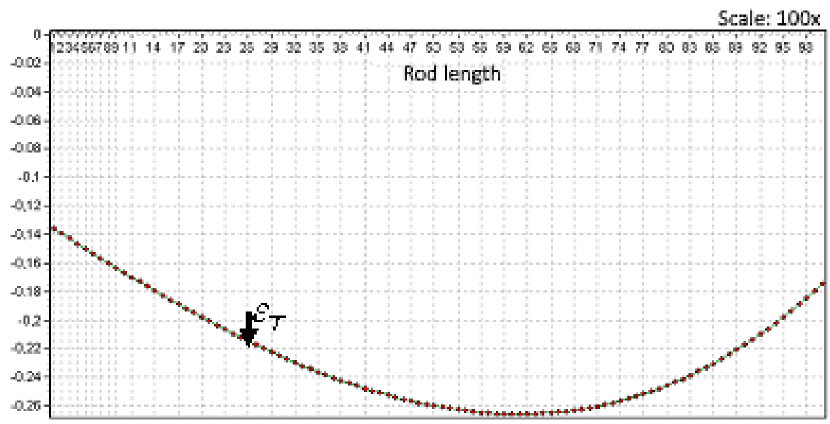

Figure 17. Fields of distribution of the value of one hundred nodal deformations from the temperature ε_T along the length of the rod

Thus, when calculating the thermal strength of rods of limited length clamped by two ends under action of the heat flux on the lateral surface changing along the coordinate, in order to obtain high-precision numerical results, it is necessary to discretise at least ten quadratic finite elements. After testing the developed mathematical model and the corresponding computational algorithm, the effect of the length of the rod on the thermo-stressed state was analysed. To do this, the values of the compressive force $R,(kg(f))$ and the effective stress $\sigma,(kg(f)/cm^2)$ were calculated for different values of the rod length. These results are shown in Table 6.

Table 6. The effect of the length of the rod on the thermo-stressed state of the investigated rod

No.	$L(cm)$	$R,(kg(f))$	$\sigma,(kg(f)/cm^2)$	%
1	30	-56454.58	-4494.79	100
2	27	-47446.29	-3769.61	83.86
3	24	-39522.13	-3146.66	70
4	21	-32893.79	-2618.93	58.26
5	18	-27272.95	-2179.375	48.48
6	15	-22871.3	-1820.96	40.5

In addition, the thermal stress-strain state of the rod under consideration is influenced by the value of the heat transfer coefficient $h,(W/cm^2 \cdot C)$ between the material of the rod and the surrounding cross-sectional area of the clamped ends of the rod. This dependence on a specific example is shown in Table 7.

Table 7. Influence of the heat transfer coefficient on the thermo-stressed state of the investigated rod

No.	$h,(W/cm^2 \cdot^{\circ} C)$	$R,(kg(f))$	$\sigma,(kg(f)/cm^2)$	%
1	10	-56454.58	-4494.79	100
2	9	-59332.916	-4723.958	105.1
3	8	-62930.83	-5010.41	111.47
4	7	-67556.72	-5378.72	119.66
5	6	-73724.583	-5869.79	130.59
6	5	-82359.583	-6557.29	145.88

It should be noted that the thermo-stressed state of the investigated rod is also influenced by the value of the ambient temperature$(T_a,^0 C)$. These dependencies are shown in Table 8.

Table 8. Influence of ambient temperature on the thermo-stressed state of the investigated rod

No.	$(T_a,^0 C)$	$(R,kg(f))$	$\left(\sigma,\frac{kg(f)}{cm^2}\right)$	%
1	40	-56454.58	-4494.79	100
2	35	-54884.58	-4369.79	97.22
3	30	-53314.58	-4244.79	94.438
4	25	-51744.58	-4119.79	91.657
5	20	-50174.58	-3994.79	88.876

4. Conclusion

Thus, a mathematical model and a corresponding computational algorithm for the numerical simulation of the thermo-stressed state of a rod clamped by two ends under influence of a heat flow on the lateral surface were developed. It has been proven that in order to obtain high-precision numerical results, it is necessary to discretise at least ten quadratic finite elements, then the calculation error does not exceed 0.00163%. When solving this problem, it was also found:

a) with a decrease in the length of the rod, the values of the compressive force (R) and the effective stress (σ) decrease in a nonlinear manner. In particular, with a decrease in the length of the rod by 10, 20, 30, 40 and 50%, the values of R and σ decrease by 16.14; 30; 41.74; 51.52 & 59.5%, respectively;
b) with a decrease in the value of the heat transfer coefficient in this example by 10, 20, 30, 40, and 50% leads to an increase in the values of the compressive force (R) and effective stress (σ), respectively, by 5.1; 11.47; 19.66; 30.59, and 45.88%;
c) with a decrease in the temperature value of the surrounding area of the cross-sections of the two clamped ends of the medium rod by 12.5; 25; 37.5, and 50% leads to a decrease in the values of the compressive force (R) and effective stress (σ), respectively, by 2.78; 5.562; 8.343, and 11.124%.

References

[1] H.-F. Li, J. Zhao, C.-Q. Cheng, X.-H. Min, T.-S. Cao, and J. Xu, "Prediction of High Temperature Creep Deformation and Rupture Life on HP Heat Resistant Alloy Using Zc Parameter," *Cailiao Gongcheng/Journal of Materials Engineering*, vol. 46, no. 3, pp. 112-116, 2018.

[2] B. Meng, K. Yang, J. Wu, and X. Zhang, "Preparation Method of High Conductivity and Heat Resistant Aluminum Alloy," *Tezhong Zhuzao Ji Youse Hejin/Special Casting and Nonferrous Alloys*, vol. 39, no. 8, pp. 922-924, 2019.

[3] J. Wang, "Kinetic and Strength Calculation of Age-Hardening Phases in Heat-Resistant Aluminum Alloys with Silver," *Materials Science Forum*, vol. 993 MSF, pp. 1051-1056, 2020.

[4] A. M. Adaskin, A. K. Kirillov, and A. A. Kutin, "Improving the Cutting of Heat-Resistant Chromium Alloy," *Russian Engineering Research*, vol. 40, no. 9, pp. 748-750, 2020.

[5] P. G. Min, V. V. Sidorov, V. E. Vadeev, and V. V. Kramer, "Development of Corrosion and Heat-Resistant Nickel Alloys and their Production Technology with the Aim of Import Substitution," *Power Technology and Engineering*, vol. 54, no. 2, pp. 225-231, 2020.

[6] N. V. Petrushin, A. G. Evgenov, A. V. Zavodov, and I. A. Treninkov, "Structure and Strength of the ZhS32-VI Heat-Resistant Nickel Alloy Produced by the Method of Selective Laser Alloying on a Single-Crystal Substrate," *Inorganic Materials: Applied Research*, vol. 9, no. 4, pp. 620-627, 2018.

[7] N. Zhang, R. Cheng, H. Dong, W. Liu, J. Zhan, B. Jiang, and F. Pan, "Application and Research Progress of Strontium in Heat-resistant Magnesium Alloy," *Cailiao Daobao/Materials Reports*, vol. 33, no. 8, pp. 2565-2571, 2019.

[8] G. Li, H. Liao, X. Suo, Y. Tang, U.S. Dixit, and P. Petrov, "Cr-Induced Morphology Change of Primary Mn-Rich Phase in Al-Si-Cu-Mn Heat Resistant Aluminum Alloys and Its Contribution to High Temperature Strength," *Materials Science and Engineering A*, vol. 709, pp. 90-96, 2018.

[9] G.-Z. Quan, K.-K. Zhang, C. An, H.-M. Qiu, and Y.-F. Xia, "Analysis of Dynamic Recrystallization Behaviors in Resistance Heating Compressions of Heat-Resistant Alloy by Multi-Field and Multi-Scale Coupling Method," *Computational Materials Science*, vol. 149, pp. 73-83, 2018.

[10] X. Xu, X. Jin, Z. Liu, B. Zhang, R. Zhang, Y. Zhuang, P. Zhang, and H. Wei, "Microstructure and Properties of a New Al-Cu-Mg-Zn-Zr-Ti Heat Resistant Aluminum Alloy," *Materials Research Express*, vol. 6, no. 12, article number 1265H8, 2019.

[11] A. Facco, M. Couvrat, D. Magné, M. Roussel, A. Guillet, and C. Pareige, "Microstructure Influence on Creep Properties of Heat-Resistant Austenitic Alloys with High Aluminum Content," *Materials Science and Engineering A*, vol. 783, article number 139276, 2020.

[12] Y. H. Kvasnytska, L. M. Ivaskevych, O. I. Balytskyi, I. I. Maksyuta, and H. P. Myalnitsa, "High-Temperature Salt Corrosion of a Heat-Resistant Nickel Alloy," *Materials Science*, vol. 56, no. 3, pp. 432-440, 2020.

[13] I. A. Sustaita-Torres, S. Haro-Rodríguez, and R. Colás, "Aging of a Low Carbon Heat Resistant Cast Alloy," *High Temperature Materials and Processes*, vol. 37, no. 2, pp. 133-139, 2018.

[14] P. V. Patrin, B. V. Karpov, A. S. Aleshchenko, and S. P. Galkin, "Capability Process Assessment of Radial-Displacement Rolling of Heat-Resistant Alloy HN73MBTYU," *Steel in Translation*, vol. 50, no. 1, pp. 42-45, 2020.

[15] H. Liao, Q. Liu, G. Li, and U. S. Dixit, "Effect of Ni Addition on The Solidification Process and Microstructure of Al-12%Si-4%Cu-1.2%Mn-X%Ni Heat-Resistant Alloys," *Minerals, Metals and Materials Series*, Part F4, pp. 267-678, 2018.

[16] Y. Fu, Y. Zhuang, X. Xu, J. Zhang, Z. Liu, B. Zhang, X. Jin, R. Zhang, P. Zhang, and H. Wei, "Effect of Ti Content and Hot/Cold Extrusion on Microstructure and Properties Of 2219 Heat-Resistant Aluminum Alloy," *Materials Research Express*, vol. 6, no. 10, article number 1065F2, 2019.

[17] J. Fang, Y. Huang, G. Yu, and Z. Hu, "Influence of Cold Deformation on Properties and Static Recrystallization of Al-Mg-Si-Zr Heat-Resistant Aluminum Alloy," *Jinshu Rechuli/Heat Treatment of Metals*, vol. 44, no. 8, pp. 37-40, 2019.

[18] H.-S. Bao, G. Yang, Z.-Z. Chen, and Z.-D. Liu, "Effects of Long-Term Aging on Microstructure and Properties of a Tungsten Bearing Heat-Resistant Alloy," *Journal of Iron and Steel Research International*, vol. 27, no. 4, pp. 477-487, 2020.

[19] B. Kenzhegulov, N. Shazhdekeyeva, A. N. Myrzhasheva, G. T. Kabylhamitov, and R. U. Tuleuova, "Necessary Optimality Conditions for Determining of The Position of The Boundary of Oil Deposit," *International Journal of Engineering Research and Technology*, vol. 13, pp. 1204-1209, 2020.

[20] B. Kenzhegulov, J. Kultan, D. B. Alibiyev, and A. Sh. Kazhikenova, "Numerical Modelling of Thermomechanical Processes in Heat-Resistant Alloys," *Bulletin of the Karaganda University. Physics Series*, vol. 2, no. 98, pp. 101-107, 2020.

[21] B. Kenzhegulov, N. Shazhdekeyeva, A. N. Myrzhasheva, and R. U. Tuleuova, "A Numerical Method for Determining the Dependence of The Thermally Stressed State of a Rod on Ambient Temperature with The Simultaneous Presence of Thermal Processes," *Periodico Tche Quimica*, vol. 17, pp. 765-780, 2020.

[22] V. A. Zagovorchev, and O. V. Tushavina, "The Use of Jet Penetrators for Movement in The Lunar Soil," *INCAS Bulletin*, vol. 11, pp. 121-130, 2019.

[23] V. A. Zagovorchev, and O. V. Tushavina, "Selection of Temperature and Power Parameters for Multi-Modular Lunar Jet Penetrator," *INCAS Bulletin*, vol. 11, Special Issue, pp. 231-241, 2019.

[24] S. Vakhneev, and E. Starovoitov, "Damping of Circular Composite Viscoelastic Plate Vibration Under Neutron Irradiation," *Journal of Applied Engineering Science*, vol. 18, no. 4, pp. 699-704, 2020.

[25] Y. Sun, M. Y. Kuprikov, and E. L. Kuznetsova, "Effect of Flight Range on The Dimension of The Main Aircraft," *INCAS Bulletin*, vol. 12, Special Issue, pp. 201-209, 2020.

[26] Y. Li, A. M. Arutiunian, E. L. Kuznetsova, and G. V. Fedotenkov, "Method for Solving Plane Unsteady Contact Problems for Rigid Stamp and Elastic Half-Space with A Cavity of Arbitrary Geometry and Location," *INCAS Bulletin, vol.* 12, Special Issue, pp. 99-113, 2020.

[27] E. L. Kuznetsova, G. V. Fedotenkov, and E. I. Starovoitov, "Methods of Diagnostic of Pipe Mechanical Damage Using Functional Analysis, Neural Networks and Method of Finite Elements," *INCAS Bulletin*, vol. 12, Special Issue, pp. 79-90, 2020.

[28] V. A. Pogodin, L. N. Rabinskii, and S. A. Sitnikov, "3D Printing of Components for The Gas-Discharge Chamber of Electric Rocket Engines," *Russian Engineering Research,* vol. 39, no. 9, pp. 797-799, 2019.

[29] N. S. Severina, "Software Complex for Solving the Different Tasks of Physical Gas Dynamics," *Periodico Tche Quimica*, vol. 16, no. 32, pp. 424-436, 2019.

[30] A. V. Babaytsev, L. N. Rabinskiy, and K. T. Aung, “Investigation of The Contact Zone of a Cylindrical Shell Located Between Two Parallel Rigid Plates with A Gap,” *INCAS Bulletin*, vol. 12, Special Issue, pp. 43-52, 2020.

[31] A. V. Babaytsev, and L. N. Rabinskiy, “Design Calculation Technique for Thick-Walled Composite Constructions Operating Under High-Speed Loading,” *Periodico Tche Quimica*, vol. 1, no. 33, pp. 480-489, 2019.

[32] R. Dinzhos, N. Fialko, V. Prokopov, Y. Sherenkovskiy, N. Meranova, N. Koseva, V. Korzhik, O. Parkhomenko, and N. Zhuravskaya, “Identifying the Influence of The Polymer Matrix Type on The Structure Formation of Microcomposites When They Are Filled with Copper Particles,” *Eastern-European Journal of Enterprise Technologies*, vol. 5, no. 6-107, pp. 49-57, 2020.

[33] A. V. Babaytsev, Y. K. Kyaw, S. N. Vakhneev, and T. Zin Hein, “Study of The Influence of Spherical Inclusions on Mechanical Characteristics,” *Periodico Tche Quimica, vol.* 17, no. 35, pp. 654-662, 2020.

[34] N. M. Fialko, V. G. Prokopov, N. O. Meranova, Yu. S. Borisov, V. N. Korzhik, and G. P. Sherenkovskaya, “Heat Transport Processes in Coating-Substrate Systems Under Gas-Thermal Deposition,” *Fizika i Khimiya Obrabotki Materialov*, vol. 2, pp. 68-75, 1994.

[35] A. V. Babaytsev, and A. A. Zotov, “Designing and Calculation of Extruded Sections of An Inhomogeneous Composition,” *Russian Metallurgy (Metally)*, vol. 2019, no. 13, pp. 1452-1455, 2019.

[36] R. Navrodska, N. Fialko, G. Presich, G. Gnedash, S. Alioshko, and S. Shevcuk, “Reducing Nitrogen Oxide Emissions in Boilers at Moistening of Blowing Air in Heat Recovery Systems,” *E3S Web of Conferences*, vol. 100, article number 00055, 2019.

[37] A. V. Babaytsev, A. A. Orekhov, and L. N. Rabinskiy, “Properties and Microstructure of Alsi10mg Samples Obtained by Selective Laser Melting,” *Nanoscience and Technology*, vol. 11, no. 3, pp. 213-222, 2020.

[38] N. M. Fialko, R. O. Navrodska, S. I. Shevchuk, and G. O. Gnedash, “The Environmental Reliability of Gas-Fired Boiler Units by App Lying Modern Heat-Recovery Technologies,” *Naukovyi Visnyk Natsionalnoho Hirnychoho Universytetu*, vol. 2020, no. 2, pp. 96-100, 2020.

[39] R. V. Dinzhos, N. M. Fialko, and E. A. Lysenkov, “Analysis of The Thermal Conductivity of Polymer Nanocomposites Filled with Carbonnanotubes and Carbon Black,” *Journal of Nano- and Electronic Physics*, vol. 6, no. 1, article number 01015, 2014.

[40] V. V. Bodryshev, A. V. Babaytsev, and L. N. Rabinskiy, “Investigation of Processes of Deformation of Plastic Materials with The Help of Digital Image Processing,” *Periodico Tche Quimica*, vol. 16, no. 33, pp. 865-876, 2019.

[41] V. A. Korolenko, Y. Li, V. N. Dobryanskiy, and Y. O. Solyaev, “Experimental Studies and Modelling of Fracture Toughness of The Epoxy Samples with Eccentric Cracks,” *Journal of Applied Engineering Science*, vol. 18, no. 4, pp. 719-723, 2020.

[42] M. Sha, O. A. Prokudin, Y. O. Solyaev, and S. N. Vakhneev, “Dependence of Glare Destruction Mechanisms on The Elongation of Samples in Tests to Three-Point Flexural,” *Periodico Tche Quimica*, vol. 17, no. 35, pp. 549-558, 2020.

[43] A. Babaytsev, V. Dobryanskiy, and Y. Solyaev, “Optimization of Thermal Protection Panels Subjected to Intense Heating and Mechanical Loading,” *Lobachevskii Journal of Mathematics*, vol. 40, no. 7, pp. 887-895, 2019.

[44] S. A. Lurie, P. A. Belov, Y. O. Solyaev, and E. C. Aifantis, “On One Class of Applied Gradient Models with Simplified Boundary Problems,” *Materials Physics and Mechanics*, vol. 32, no. 3, pp. 353-369, 2017.

[45] Yu. G. Evtushenko, V. I. Zubov, S. A. Lurie, and Yu. O. Solyaev, “Identification of Kinetic Parameters of The Model of Interphase Layer Growth in A Fibrous Composite,” *Composites: Mechanics, Computations, Applications*, vol. 7, no. 3, pp. 175-187, 2016.

[46] I. A. Kapitonov, "Legal Support for Integration of Renewable Energy Sources in The Energy Law of The Countries from The International Legal Position," *Kuwait Journal of Science,* vol. 46, no. 1, pp. 68-75, 2019.

[47] D. Topchiy, and A. Bolotova, "Assessment and Inspection of The Technical Condition of Monolithic Reinforced Structures in Transportation Infrastructure Facilities," *Journal of Physics: Conference Series,* vol. 1425, no. 1, article number 012005, 2020.

[48] E. L. Kuznetsova, and A. V. Makarenko, "Mathematic Simulation of Energy-Efficient Power Supply Sources for Mechatronic Modules of Promising Mobile Objects," *Periodico Tche Quimica,* vol. 15, Special Issue 1, pp. 330-338, 2018.

[49] I. A. Kapitonov, "Development of Low-Carbon Economy as The Base of Sustainable Improvement of Energy Security," *Environment, Development and Sustainability,* vol. 23, no. 3, pp. 3077-3096, 2021.

[50] A. Zvorykin, N. Fialko, S. Julii, S. Aleshko, N. Meranova, M. Hanzha, I. Bashkir, S. Stryzheus, A. Voitenko, and I. Pioro, "CFD Study on Specifics of Flow and Heat Transfer in Vertical Bare Tubes Cooled with Water at Supercritical Pressures," *International Conference on Nuclear Engineering, Proceedings, ICONE,* vol. 9, pp. 1-13, 2017.

[51] V. G. Prokopov, N. M. Fialko, G. P. Sherenkovskaya, V. L. Yurchuk, Yu. S. Borisov, A. P. Murashov, and V. N. Korzhik, "Effect of Coating Porosity on The Process of Heat Transfer with Gas-Thermal Deposition," *Powder Metallurgy and Metal Ceramics,* vol. 32, no. 2, pp. 118-121, 1993.

[52] A. Zvorykina, S. Gupta, W. Peiman, I. Pioro, and N. Fialko, "Current Status and Future Applications Of Supercritical Pressures In Power Engineering," *International Conference on Nuclear Engineering, Proceedings, ICONE,* vol. 5, no. 1, pp. 285-300, 2012.

[53] N. Fialko, R. Navrodska, M. Ulewicz, G. Gnedash, S. Alioshko, and S. Shevcuk, "Environmental Aspects of Heat Recovery Systems of Boiler Plants," *E3S Web of Conferences,* vol. 100, article number 00015, 2019.

[54] A. Lapidus, and A. Makarov, "Statistical Learning Problem of Artificial Neural Network to Control Roofing Process," *MATEC Web of Conferences,* vol. 117, article number 00100, 2017.

[55] I. A. Kapitonov, V. G. Korolev, A. A. Shadrin, and A. A. Shulus, "The Role of Small and Medium-Sized Innovative Enterprises in The Solution of The Import Substitution Task in Oil and Gas-Sector Segment of The Russian Fuel and Energy Complex," *International Journal of Energy Economics and Policy*, vol. 7, no. 3, pp. 137-145, 2017.

[56] S. A. Montayev, A. B. Shinguzhiyeva, N. B. Adilova, A. S. Montayeva, and A. S. Montayeva, "Development of Effective Technological Parameters for Formation of a Porous Structure of The Raw Composition in Order to Obtain a Lightweight Granular Insulation Material," *ARPN Journal of Engineering and Applied Sciences,* vol. 11, no. 17, pp. 10454-10459, 2016.

[57] I. A. Kapitonov, "Low-Carbon Economy as The Main Factor of Sustainable Development of Energy Security," *Industrial Engineering and Management Systems,* vol. 19, no. 1, pp. 3-13, 2020.

[58] I. A. Kapitonov, and V. I. Voloshin, "Strategic Directions for Increasing the Share of Renewable Energy Sources in The Structure of Energy Consumption," *International Journal of Energy Economics and Policy*, vol. 7, no. 4, pp. 90-98, 2017.

[59] Y. K. Kyaw, E. L. Kuznetsova, and A. V. Makarenko, "Complex Mathematical Modelling of Mechatronic Modules of Promising Mobile Objects," *INCAS Bulletin,* vol. 12, Special Issue, pp. 91-98, 2020.

[60] N. M. Fialko, R. O. Navrodska, G. O. Gnedash, G. O. Presich, and S. I. Shevchuk, "Study of Heat-Recovery Systems of or Heating and Moisturing Combustion Air of Boiler Units," *Science and Innovation*, vol. 16, no. 3, pp. 43-49, 2020.

[61] A. Lapidus, A. Khubaev, and T. Bidov, "Development of A Three-Tier System of Parameters in The Formation of The Organizational and Technological Potential of Using Non-Destructive Testing Methods," *E3S Web of Conferences,* vol. 97, article number 06037, 2019.

[62] D. Topchiy, and A. Bolotova, “Studying Specific Features of The Monolithic Construction Technology Based on Systemic Analysis,” *IOP Conference Series: Materials Science and Engineering,* vol. 603, no. 5, article number 052004, 2019.

[63] N. I. Kobasko, N. M. Fialko, and N. O. Meranova, “Numerical Determination of The Duration of The Nucleate-Boiling Phase in The Course of Steel-Plate Hardening,” *Heat Transfer. Soviet Research,* vol. 16, no. 2, pp. 130-135, 1984.

[64] A. A. Skvortsov, S. M. Zuev, and M. V. Koryachko, “Contact Melting of Aluminum-Silicon Structures Under Conditions of Thermal Shock,” *Key Engineering Materials,* vol. 771, pp. 118-123, 2018.

[65] I. A. Kapitonov, G. A. Taspenova, V. R. Meshkov, and A. A. Shulus, “Integration of Small and Middle-Sized Enterprises into Large Energy Corporations as A Factor of Business Sustainability,” *International Journal of Energy Economics and Policy,* vol. 7, no. 2, pp. 44-52, 2017.

[66] I. A. Kapitonov, V. I. Voloshin, and V. G. Korolev, “Eastern Vector of Russian State Policy Development for Ensuring Energy Security,” *International Journal of Energy Economics and Policy,* vol. 8, no. 5, pp. 335-341, 2018.

[67] G. A. Ganiyeva, B. R. Ryskulova, and S. Sh. Tashpulatov, “Ergonomic Studies of Dynamic Compliance of Parameters Within the Man-Special Clothing System for Workers of The Oil Industry,” *Izvestiya Vysshikh Uchebnykh Zavedenii, Seriya Teknologiya Tekstil'noi Promyshlennosti,* vol. 2015, no. 3, pp. 151-154, 2015.

[68] D. V. Topchiy, A. S. Bolotova, A. A. Zelentsov, A. S. Vorobev, and A. V. Atamanenko, “Technical Rationing of The Construction Technology of Reinforced Concrete Floor Slabs Using Non-Removable Empitness-Liners,” *International Journal of Civil Engineering and Technology,* vol. 10, no. 2, pp. 2160-2166, 2019.

[69] I. A. Kapitonov, T. G. Filosofova, and V. G. Korolev, “Development Of Digital Economy in the Energy Industry-Specific Modernization,” *International Journal of Energy Economics and Policy,* vol. 9, no. 4, pp. 273-282, 2019.

[70] A. Zvorykin, S. Aleshko, N. Fialko, N. Maison, N. Meranova, A. Voitenko, and I. Pioro, “Computer Simulation of Flow and Heat Transfer in Bare Tubes at Supercritical Parameters,” *International Conference on Nuclear Engineering, Proceedings, ICONE,* vol. 5, pp. 1-12, 2016.

[71] S. A. Montayev, B. T. Shakeshev, M. Z. Ryskaliyev, N. B. Adilova, and K. A. Narikov, “Collagen Agent Technology for Foam Concrete Production,” *ARPN Journal of Engineering and Applied Sciences,* vol. 12, no. 5, pp. 1674-1678, 2017.

[72] S. A. Montayev, S. M. Zharylgapov, K. A. Bisenov, B. T. Shakeshev, and M. Z. Almagambetova, “Investigating Oil Sludges and Their Application as Energy Efficient and Modifying Component in Ceramic Pastes,” *Research Journal of Pharmaceutical, Biological and Chemical Sciences,* vol. 7, no. 3, pp. 2407-2415, 2016.

[73] A. A. Lapidus, and A. N. Makarov, “Model for The Potential Manufacture of Roof Structures for Residential Multi-Storey Buildings,” *Procedia Engineering,* vol. 153, pp. 378-383, 2016.

[74] I. A. Kapitonov, V. I. Voloshin, and V. G. Korolev, “Energy Security of Territories as A Factor of Sustainable Development Under the Conditions of Economic Changes,” *International Journal of Energy Economics and Policy,* vol. 9, no. 6, pp. 210-221, 2019.

[75] S. A. Montayev, N. S. Montayeva, A. B. Shinguzhiyeva, K. Zhanabaevichdosov, and M. Zhanaidarovichryskaliyev, “Possibility of Producing Sintered Fine Porous Granulated Ceramic Filler Using Ash of Thermal Power Stations in Combination with Clay Rocks,” *International Journal of Mechanical and Production Engineering Research and Development,* vol. 9, no. 4, pp. 1087-1096, 2019.

[76] G. A. Ganiyeva, B. R. Ryskulova, and S. S. Tashpulatov, "Selection of Special Clothes Design Parameters on The Basis of Optimisation of Dynamic Conformance Parameters," *International Journal of Applied Engineering Research,* vol. 10, no. 19, pp. 40603-40606, 2015.

[77] I. Cherunova, S. Tashpulatov, and Y. Davydova, "Geometric Conditions of Mathematical Modeling of Human Heat Exchange Processes with The Environment for CAD Systems Creating Heat-Shielding Clothing," *IOP Conference Series: Materials Science and Engineering,* vol. 680, no. 1, article number 012039, 2019.

[78] V. N. Korzhyk, L. D. Kulak, V. E. Shevchenko, V. V. Kvasnitskiy, N. N. Kuzmenko, X. Liu, Y. X. Cai, L. Wang, H. W. Xie, and L. M. Zou, "New Equipment for Production of Super Hard Spherical Tungsten Carbide and Other High-Melting Compounds Using the Method of Plasma Atomization of Rotating Billet," *Materials Science Forum,* vol. 898, pp. 1485-1497, 2017.

[79] D. Topchiy, and A. Bolotova, "Systematization of Factors Affecting the Organizational Processes in The Conversion of Buildings," *IOP Conference Series: Materials Science and Engineering,* vol. 753, no. 3, article number 032042, 2020.

[80] D. G. Blinov, V. G. Prokopov, Yu. V. Sherenkovskii, N. M. Fialko, and V. L. Yurchuk, "Simulation of Natural Convection Problems Based on Low-Dimensional Model," *International Communications in Heat and Mass Transfer,* vol. 29, no. 6, pp. 741-747, 2002.

[81] I, Katranov, and A. Lapidus, "Mobile Building Life Cycle," *MATEC Web of Conferences,* vol. 193, article number 03011, 2018.

[82] A. Lapidus, and D. Topchiy, "Construction Supervision at The Facilities Renovation," *E3S Web of Conferences,* vol. 91, article number 08044, 2019.

[83] I. A. Kapitonov, "Transformation of Social Environment in The Application of Alternative Energy Sources," *Environment, Development and Sustainability,* vol. 22, no. 8, pp. 7683-7700, 2020.

[84] A. Z. Skorokhod, I. S. Sviridova, and V. N. Korzhik, "Structural and Mechanical Properties of Polyethylene Terephthalate Coatings as Affected by Mechanical Pretreatment of Powder in The Course of Preparation," *Mekhanika Kompozitnykh Materialov,* vol. 30, no. 4, pp. 455-463, 1994.

[85] I. Cherunova, S. Tashpulatov, and A. Merkulova, "Development of Automation Algorithm for Step of Designing Technology of Static Electricity Protection Clothing," *2018 International Russian Automation Conference, RusAutoCon 2018,* vol. 1, article number 8501821, 2018.

[86] R. V. Dinzhos, E. A. Lysenkov, and N. M. Fialko, "Influence of Fabrication Method and Type of The Filler on The Thermal Properties of Nanocomposites Based on Polypropylene," *Voprosy Khimii i Khimicheskoi Tekhnologii,* vol. 2015, no. 5, pp. 56-62, 2015.

[87] Yu. S. Borisov, V. E. Oliker, E. A. Astakhov, V. N. Korzhik, and Yu. A. Kunitskii, "Structure and Properties of Gas-Thermal Coatings of Fe-B-C and Fe-Ti-B-C alloys," *Soviet Powder Metallurgy and Metal Ceramics,* vol. 26, no. 4, pp. 313-318, 1987.

[88] A. Lapidus, T. Bidov, and A. Khubaev, "The Study of The Calibration Dependences Used When Testing the Concrete Strength by Nondestructive Methods," *MATEC Web of Conferences,* vol. 117, article number 00094, 2017.

[89] A. Lapidus, and I. Abramov, "Studying the Methods for Determining and Maintaining Sustainability of a Construction Firm," *MATEC Web of Conferences,* vol. 251, article number 05017, 2018.

[90] S. A. Mizuriaev, S. A. Montaev, and A. T. Taskaliev, "Artificial Broken Stone Production for Industrial and Civil Engineering: Technological Parameters," *Procedia Engineering,* vol. 111, pp. 534-539, 2015.

[91] A. Jurgaitis, D. Topchiy, A. Kravchuk, and D. Shevchuk, "Controlling Methods of Buildings' Energy Performance Characteristics," *E3S Web of Conferences,* vol. 91, article number 02026, 2019.

[92] V. Toporovskiy, A. Kudryashov, V. Samarkin, J. Sheldakova, A. Rukosuev, A. Skvortsov, and D. Pshonkin, "Bimorph Deformable Mirror with A High Density of Electrodes to Correct for Atmospheric Distortions," *Applied Optics*, vol. 58, no. 22, pp. 6019-6026, 2019.

[93] D. Topchiy, and A. Tokarskiy, "Formation of Hierarchies in The System of Organization of State Construction Supervision in Case of Reorientation of Urban Areas," *Communications in Computer and Information Science* vol. 1046, pp. 134-143, 2019.

[94] S. A. Montayev, A. S. Montayeva, N. B. Adilova, A. B. Shinguzhiyeva, N. S. Montayeva, and A. T. Taskaliyev, "Prospects of Creating the Technology of Composite Adsorbent for Water Purification Based on The Composition of Siliceous and Clay Rocks of Kazakhstan," *International Journal of Mechanical Engineering and Technology*, vol. 9, no. 1, pp. 805-813, 2018.

[95] H. Yuilin, A. Beljatynskij, and A. Ishchenko, "Non-Roundabout Design of Cancel the Intersection Signal Light on Horizontal Plane," *E3S Web of Conferences*, vol. 91, article number 05003, 2019.

[96] I. V. Cherunova, S. S. Tashpulatov, and S. V. Kurenova, "Treated Textile Electrostatic Properties Study," *Materials Science Forum*, vol. 992, pp. 439-444, 2020.

[97] I. Cherunova, S. Tashpulatov, and S. Kolesnik, "Automation of Deformed Fibrous Materials Thermal Characteristics Accounting Process in Garments Production," *2018 International Russian Automation Conference, RusAutoCon 2018*, article number 8501795, 2018.

[98] S. A. Montaev, N. B. Adilova, N. S. Montaeva, K. Z. Dosov, and A. A. Taudaeva, "Study of Raw Materials with The Aim of Obtaining Ceramic Filler and Heat-Insulating and Structural Wall Ceramicsm," *International Journal of Mechanical and Production Engineering Research and Development*, vol. 9, no. 5, pp. 1057-1064, 2019.

[99] G. M. Grigorenko, L. I. Adeeva, A. Y. Tunik, V. N. Korzhik, L. K. Doroshenko, Y. P. Titkov, and A. A. Chaika, "Structurization of Coatings in the Plasma Arc Spraying Process Using B_4C + (Cr, Fe)$_7C_3$-Cored Wires," *Powder Metallurgy and Metal Ceramics*, vol. 58, no. 5-6, pp. 312-322, 2019.

[100] S. Peleshenko, V. Korzhyk, O. Voitenko, V. Khaskin, and V. Tkachuk, "Analysis of The Current State of Additive Welding Technologies for Manufacturing Volume Metallic Products (Review)," *Eastern-European Journal of Enterprise Technologies*, vol. 3, no. 1-87, pp. 42-52, 2017.

[101] A. Beljatynskij, O. Prentkovskis, and J. Krivenko, "The Experimental Study of Shallow Flows of Liquid on The Airport Runways and Automobile Roads," *Transport*, vol. 25, no. 4, pp. 394-402, 2010.

[102] Y. Borisov, V. Korzhyk, and S. Revo, "Electric and Magnetic Properties of Thermal Spray Coatings with An Amorphous Structure," *Proceedings of the International Thermal Spray Conference*, vol. 1, pp. 687-691, 1998.

[103] A. Bieliatynskyi, E. Krayushkina, and A. Skrypchenko, "Modern Technologies and Materials for Cement Concrete Pavement's Repair," *Procedia Engineering*, vol. 134, pp. 344-347, 2016.

[104] N. M. Fialko, V. G. Prokopov, N. O. Meranova, Yu. S. Borisov, V. N. Korzhik, and G. P. Sherenkovskaya, "Heat Transport Processes in Coating-Substrate Systems Under Gas-Thermal Deposition," *Fizika i Khimiya Obrabotki Materialov*, vol. 2, pp. 68-75, 1994.

[105] M. Y. Kharlamov, I. V. Krivtsun, V. N. Korzhyk, Y. V. Ryabovolyk, and O. I. Demyanov, "Simulation of Motion, Heating, And Breakup of Molten Metal Droplets in The Plasma Jet at Plasma-Arc Spraying," *Journal of Thermal Spray Technology*, vol. 24, no. 4, pp. 659-670, 2015.

[106] S. Oleksandra, K. Krayushkina, T. Khymerik, and B. Andrii, "Method of Increasing the Roughness of The Existing Road," *Procedia Engineering*, vol. 165, pp. 1766-1770, 2016.

[107] D. Topchiy, and A. Bolotova, 'Risk Management in Monolithic Construction," *IOP Conference Series: Materials Science and Engineering*, vol. 962, no. 2, article number 022078, 2020.

[108] N. I. Dorogov, I. A. Kapitonov, and N. T. Batyrova, “The Role of National Plans in Developing the Competitiveness of The State Economy,” *Entrepreneurship and Sustainability Issues*, vol. 8, no. 1, pp. 672-686, 2020.

[109] G. M. Hryhorenko, L. I. Adeeva, A. Y. Tunik, M. V. Karpets, V. N. Korzhyk, M. V. Kindrachuk, and O. V. Tisov, “Formation of Microstructure of Plasma-Arc Coatings Obtained Using Powder Wires with Steel Skin and B4C + (Cr, Fe)7C3 + Al Filler,” *Metallofizika i Noveishie Tekhnologii*, vol. 42, no. 9, pp. 1265-1282, 2020.

[110] M. Starikov, A. Beljatynskij, O. Prentkovskis, and I. Klimenko, “The Use of Magnetic Coercivity Method to Diagnose Crane Metalware,” *Transport*, vol. 26, no. 3, pp. 255-262, 2011.

[111] S. A. Mizuriaev, S. A. Montaev, and A. B. Shinguzhieva, “On Effectiveness of Low-Bloating Raw Materials Use (E.G., Loam) In Concrete Aggregate,” *Procedia Engineering*, vol. 111, pp. 530-533, 2015.

[112] B. Kovačic, R. Kamnik, and A. Bieliatynskyi, “The Different Methods of Displacement Monitoring at Loading Tests of Bridges or Different Structures,” *MATEC Web of Conferences*, vol. 53, article number 01048, 2016.

[113] S. A. Montayev, N. B. Adilova, S. M. Zharylgapov, A. S. Montayeva, B. T. Shakeshev, and M. Z. Ryskaliyev, “Physical and Mechanical Properties and Structure of Heat Insulating Engineering Foam Glass Derived from Mixed Waste Glass and Wollastonite Slags,” *International Journal of Mechanical Engineering and Technology*, vol. 8, no. 12, pp. 944-954, 2017.

[114] G. M. Grigorenko, L. I. Adeeva, A. Y. Tunik, V. N. Korzhik, and M. V. Karpets, “Plasma Arc Coatings Produced from Powder-Cored Wires with Steel Sheaths,” *Powder Metallurgy and Metal Ceramics*, vol. 59, no. 5-6, pp. 318-329, 2020.

[115] N. Kuzhel, A. Bieliatynskyi, O. Prentkovskis, I. Klymenko, S. Mikaliunas, O. Kolganova, S. Kornienko, and V. Shutko, “Methods for Numerical Calculation of Parameters Pertaining to The Microscopic Following-The-Leader Model of Traffic Flow: Using the Fast Spline Transformation,” *Transport*, vol. 28, no. 4, pp. 413-419, 2013.

[116] L. N. Nutfullaeva, A. F. Plekhanov, I. G. Shin, S. S. H. Tashpulatov, I. V. Cherunova, S. H. N. Nutfullaeva, and E. A. Bogomolov, “Research of Conditions of Formation Package and Ensure the Safety of The Pillows from Composite Nonwoven Fibers Materials,” *Izvestiya Vysshikh Uchebnykh Zavedenii, Seriya Teknologiya Tekstil'noi Promyshlennosti*, vol. 380, no. 2, pp. 95-101, 2019.

[117] D. A. Y. Al-Saadi, V. F. Pershin, B. N. Salimov, and S. A. Montaev, “Modification of Graphite Greases Graphene Nanostructures,” *Journal of Friction and Wear*, vol. 38, no. 5, pp. 355-358, 2017.

[118] O. V. Chernets, V. M. Korzhyk, G. S. Marynsky, S. V. Petrov, and V. A. Zhovtyansky, “Electric Arc Steam Plasma Conversion of Medicine Waste and Carbon Containing Materials,” *GD 2008 - 17th International Conference on Gas Discharges and Their Applications*, vol. 1, pp. 465-468, 2008.

[119] A. Onishchenko, L. Stolyarova, and A. Bieliatynskyi, “Evaluation of The Durability of Asphalt Concrete on Polymer Modified Bitumen,” *E3S Web of Conferences*, vol. 157, article number 06005, 2020.

[120] V. Sydorets, V. Korzhyk, V. Khaskin, O. Babych, and O. Berdnikova, “On the Thermal and Electrical Characteristics of The Hybrid Plasma-MIG Welding Process,” *Materials Science Forum*, vol. 906, pp. 63-71, 2017.

[121] M. Yu. Kharlamov, I. V. Krivtsun, and V. N. Korzhyk, “Dynamic Model of The Wire Dispersion Process in Plasma-Arc Spraying,” *Journal of Thermal Spray Technology*, vol. 23, no. 3, pp. 420-430, 2014.

[122] S. S. Tashpulatov, I. V. Cherunova, M. K. Rasulova, D. D. Inogamdjanov, M. Yu. Umarova, A. D. Daminov, U. R. Uzakova, and S. G. Jurayeva, “Development of The Calculation Method of Polymer Compound Mass to Be Applied onto The Textile Garment Pieces,” *IOP Conference Series: Materials Science and Engineering*, vol. 459, no. 1, article number 012067, 2018.

[123] O. Stepanchuk, A. Bieliatynskyi, O. Pylypenko, and S. Stepanchuk, “Peculiarities of City Street-Road Network Modelling,” *Procedia Engineering*, vol. 134, pp. 276-283, 2016.

[124] Y. Barabanshchikov, T. Belkina, A. Muratova, and A. Bieliatynskyi, “Heat Liberation of Barium Cements as A Background of Their Application in Mass Concrete Structures,” *Solid State Phenomena*, vol. 871, pp. 9-15, 2016.